

---

**A DFT Study of Diatomic Oxygen Adsorption on  
Pt(100) and Pt(111)**

**CHE4045Z Project 15**

---

By

**Michel Amato (AMTMIC001)**

**Jean-Claude Carreno (CRRJEA003)**

Supervisors:

**Professor Eric Van Steen**

**Pierre Cilliers**

**Tracey Van Heerden**

November 2017



Centre for Catalysis Research

Department of Chemical Engineering

University of Cape Town

## Synopsis

Adsorption of oxygen to platinum has various applications within the fields of heterogeneous catalysis and electro-chemistry. Research into application of oxygen based platinum catalysed reactions has gained increased attention due to possible applications within renewable energy solutions, including fuel cells and production of methanol from direct methanation. Investigation on preferred adsorption geometries and adsorption energies for oxygen on platinum surfaces at various coverages and conditions may assist this field of study and aid future platinum catalyst development.

Platinum nanoparticles are most thermodynamically stable in the truncated octahedral shape, producing two surface planes of Pt(111) and Pt(100). This study focuses on diatomic adsorption of oxygen for both Pt(111) and Pt(100) surfaces and aims to determine the preferred adsorption geometries and associated energies of diatomic oxygen adsorption at varying coverages, temperatures and oxygen partial pressures.

Adsorption of diatomic oxygen at 0.25 ML for Pt(100) and Pt(111) was investigated for all possible adsorption sites using DFT calculations. It was found that bridge adsorption site was the most stable, by comparing the Gibbs adsorption energies of all tested configurations, for both Pt(100) and Pt(111) with adsorption energies at 0 K of -1.14 eV and -0.64 eV respectively.

It was then assumed that the bridge site was preferred for all higher coverages, and used to create the initial geometries of all systems tested at higher coverages. For both surfaces, the bridge site remained stable at 0.50 ML, with adsorption energies of -2.24 eV and -1.13 eV on Pt(100) and Pt(111) respectively. The preferred adsorption site at 0.75 ML for both surfaces involved a single bridge adsorption site with two atop adsorption sites, and had energies -2.13 eV and -0.50 eV respectively. It was found that full coverage on both surfaces is not stable and therefore cannot be obtained.

The most stable geometries at each coverage for both surfaces were used to produce a phase diagram in order to illustrate the most stable adsorption systems at various conditions from 0-1000 K and 0-100 bar. Results from this study indicated that the most stable adsorption geometries at 0.75 ML for both surfaces were not thermodynamically preferred over the studied ranges. Pt(100) indicated that a coverage of 0.50 ML was thermodynamically preferred across all pressures at temperatures lower than 650 K, while 0.25 ML was favoured at temperatures between 650-700 K, and at any higher temperatures oxygen would be more stable in the gas phase. Pt(111) indicated that a coverage of 0.50 ML was thermodynamically preferred across all pressures at temperatures lower than 300 K, while At 0.25 ML was thermodynamically preferred between 300-400 K, and at higher temperatures oxygen would be more stable in the gas phase across all studied pressures.

# Contents

Synopsis .....	i
List of Tables .....	v
List of Figures .....	vi
Nomenclature .....	1
Glossary .....	2
1. Introduction.....	3
1.1 Background.....	3
1.2 Problem Statement .....	4
1.3 Scope of Study.....	4
1.4 Objectives of Study .....	4
1.5 Key Questions.....	4
2. Literature Review.....	5
2.1 Global Energy Demand.....	5
2.2 Fuel Cells and Oxygen Based Reactions.....	6
2.3 Platinum Nanoparticles and Surfaces .....	8
2.4 Studies on Oxygen Adsorption to Platinum.....	10
3. Experimental Method.....	15
3.1 Methodology Overview.....	15
3.2 Calculation of Adsorption Energy .....	15
3.3 Modelling Oxygen .....	16
3.4 Model Optimisation Overview .....	16
3.5 Lattice Parameter.....	17
3.6 Parameter Optimisation Pt(100).....	18
3.6.1 Pt(100) K-Points .....	18
3.6.2 Pt(100) Cut-Off Energy .....	19
3.6.3 Pt(100) Number of Layers .....	20
3.6.4 Pt(100) Number of Relaxed Layers .....	21
3.6.5 Pt(100) Vacuum Spacing.....	22
3.7 Parameter Optimisation Pt(111).....	23
3.7.1 Pt(111) K-Points .....	23
3.7.2 Pt(111) Cut-Off Energy .....	24
3.7.3 Pt(111) Number of Layers .....	25

3.7.4 Pt(111) Number of Relaxed Layers .....	25
3.7.5 Pt(111) Vacuum Spacing.....	26
3.8 Summary of Optimised Model for Pt(100) and Pt(111) .....	27
3.9 Determination of Preferred Adsorption Sites and Adsorption Energies.....	27
3.10 Thermodynamic Correlations .....	28
4. Results and Discussion for Pt(100) .....	31
4.1 Adsorption Energies and Preferred Adsorption Sites for Pt(100) .....	31
4.1.1 Pt(100) at 0.25 ML Coverage .....	31
4.1.2 Pt(100) at 0.50 ML Coverage .....	34
4.1.3 Pt(100) at 0.75ML Coverage .....	36
4.1.4 Pt(100) at 1.00ML Coverage .....	38
4.2 Thermodynamic Analysis of Adsorption of Diatomic Oxygen on Pt(100) .....	39
4.2.1 Overview of Thermodynamics of Adsorption of Diatomic Oxygen on Pt(100).....	39
4.2.2 Dependence of the Adsorption Geometry on Temperature on Pt(100) ....	40
4.2.3 Dependence of the Adsorption Geometry on Partial Pressure of O <sub>2</sub> on Pt(100).....	41
4.3 Phase Diagram for the Adsorption of Diatomic Oxygen on Pt(100) .....	42
5. Results and Discussion for Pt(111) .....	44
5.1 Adsorption Energies and Preferred Adsorption Sites for Pt(111) .....	44
5.1.1 Pt(111) at 0.25 ML Coverage .....	44
5.1.2 Pt(111) at 0.50 ML Coverage .....	47
5.1.3 Pt(111) at 0.75 ML Coverage .....	48
5.1.4 Pt(111) at 1.00 ML Coverage .....	50
5.2 Thermodynamic Analysis of Adsorption of Diatomic Oxygen on Pt(111) .....	50
5.2.1 Overview of Thermodynamics of Adsorption of Diatomic Oxygen on Pt(111).....	50
5.2.2 Dependence of the Adsorption Geometry on Temperature on Pt(111) ....	50
5.2.3 Dependence of the Adsorption Geometry on Pressure on Pt(111) .....	52
5.3 Phase Diagram for the Adsorption of Diatomic Oxygen on Pt(111) .....	52
Conclusion.....	55
References .....	57
Appendices.....	59

Appendix A: Top and Side Views of the Initial Geometries for All Systems Tested for Pt(111) .....	59
Appendix A1: Top and Side Views of the Initial Geometries for All Systems Tested for Pt(111) at 0.50 ML Coverage .....	59
Appendix A2: Top and Side Views of the Initial Geometries for All Systems Tested for Pt(111) at 0.75 ML Coverage .....	61
Appendix A3: Top and Side Views of the Initial Geometries for All Systems Tested for Pt(111) at 1.00 ML Coverage .....	62
Appendix B: Supervisor Meeting Minutes .....	63
Appendix B1: Minutes of Meeting One 3 October 2017 .....	63
Appendix B2: Minutes of Meeting Two 11 October 2017.....	64
Appendix B3: Minutes of Meeting Three 17 October 2017 .....	65
Appendix B4: Minutes of Meeting Four 2 November 2017 .....	66
Appendix B5: Minutes of Meeting Five 9 November 2017.....	68
Appendix B6: Minutes of Meeting Six 17 November 2017.....	70
Appendix C: Ethical Considerations.....	72
Appendix C1: Cover Letter for EBE Ethical Research Application .....	72
Appendix C2: EBE Ethical Research Application Form.....	74
Appendix D: Plagiarism Declaration Form.....	75

## List of Tables

Table 1: Comparison between calculated adsorption energies in the studies carried out by Ford, Xu & Mavrikakis (2005) and Lynch & Hu (2000) on the atomic adsorption of oxygen on Pt(111) .....	12
Table 2: Summary of the optimised parameters for the optimised models of Pt(100) and Pt(111).....	27
Table 3: Description of the geometries of all systems tested at a coverage of 0.25 ML on the Pt(100) surface and their associated adsorption energies at 0 K .....	33
Table 4: Adsorption energies at 0 K for all eight configurations tested at a coverage of 0.50 ML on the Pt(100) surface .....	36
Table 5: Adsorption energies at 0 K for all four configurations tested at a coverage of 0.75 ML on the Pt(100) surface .....	37
Table 6: Description of the geometries of all systems tested at a coverage of 0.25ML on the Pt(100) surface and their associated adsorption energies at 0 K .....	47
Table 7: Adsorption energies at 0 K for all eight configurations tested at a coverage of 0.50 ML on the Pt(111) surface .....	48
Table 8: Adsorption energies at 0 K for all four configurations tested at a coverage of 0.75 ML on the Pt(111) surface .....	49

## List of Figures

Figure 1: A plot of total global energy consumption per annum (MToE) between 2006 and 2016 (British Petroleum, 2017) .....	5
Figure 2: Breakdown of global primary energy consumption in 2016 (British Petroleum, 2017) .....	5
Figure 3: Nanoparticle shape configurations: A-Tetrahedron, B-Cubic, C-Octahedron, D-Truncated Octahedron .....	8
Figure 4: Dominant surfaces on a platinum truncated tetrahedron nanoparticle (1-Pt(111),0-Pt(100)).....	9
Figure 5: Side and top views of a Pt(111) surface showing all possible adsorption sites .....	10
Figure 6: Side and top views of a Pt(100) surface showing all possible adsorption sites .....	10
Figure 7: The method for calculating the Gibbs adsorption energy using an example of diatomic oxygen adsorbed onto a hcp site on Pt(111).....	15
Figure 8: A face-centred Pt unit cell highlighting the lattice parameter: .....	17
Figure 9: The total system energy versus lattice parameter for a Pt unit cell.....	18
Figure 10: Adsorption Energy Difference Versus Number of Irreducible K-Points for Pt(100) measured from diatomic oxygen adsorption at 0.25ML on a 2x2 Pt surface with 6 layers. Reference of 20x20x20 k-point grid .....	19
Figure 11: Adsorption Energy Difference Versus Cut-Off Energy for Pt(100) measured from diatomic oxygen adsorption at 0.25ML on a 2x2 Pt surface with 6 layers. Reference of 500eV.....	19
Figure 12: adsorption energy difference versus number of layers for Pt(100) measured from diatomic oxygen adsorption at 0.25ML on a 2x2 Pt surface with 6 layers. Reference at a 12-layered slab.....	20
Figure 13: Adsorption energy differences (meV) against the number of relaxed layers in Pt(100) measured from diatomic oxygen adsorption at 0.25ML on a 2x2 Pt surface with 6 layers. Reference at a 5 relaxed layered slab .....	21
Figure 14: A Pt(111) Surface of 6 Layers with Vacuum Spacing Included .....	22
Figure 15: Adsorption Energy Difference versus Vacuum Spacing for Pt(100) measured from diatomic oxygen adsorption at 0.25ML on a 2x2 Pt surface with 6 layers. Reference at a 14 Å slab.....	23
Figure 16: Adsorption Energy Difference Versus Number of Irreducible K-Points for Pt(111) measured from diatomic oxygen adsorption at 0.25ML on a 2x2 Pt surface with 6 layers. Reference at a 20x20x20 k-point grid .....	24
Figure 17: Adsorption Energy Difference Versus Cut-Off Difference for Pt(111) measured from diatomic oxygen adsorption at 0.25ML on a 2x2 Pt surface with 6 layers. Reference at a 500eV slab.....	24
Figure 18: Adsorption energy difference versus number of layers for Pt(111) measured from diatomic oxygen adsorption at 0.25ML on a 2x2 Pt surface with 6 layers. Reference at a 12-layered slab.....	25

Figure 19: Adsorption energy differences (meV) against the number of relaxed layers in Pt(111) measured from diatomic oxygen adsorption at 0.25ML on a 2x2 Pt surface with 6 layers. Reference at a 5 relaxed layered slab .....	26
Figure 20: Adsorption Energy Difference Versus Vacuum Spacing for Pt(111) measured from diatomic oxygen adsorption at 0.25ML on a 2x2 Pt surface with 6 layers. Reference at a 14 Å vacuum.....	27
Figure 21: A Pt(111) surface with diatomic oxygen adsorbed on a hcp site at a coverage of 0.25 ML.....	28
Figure 22: Top and side views of the initial geometries of all three possible adsorption sites tested at a coverage of 0.25 ML on the Pt(100) surface .....	31
Figure 23: Top and side views of the final geometries of all three possible adsorption sites tested at a coverage of 0.25 ML on the Pt(100) surface .....	32
Figure 24: Top and side views of the initial geometries of all eight possible bridge site configurations tested at a coverage of 0.50 ML on the Pt(100) surface.....	35
Figure 25: Top and side views of the initial geometries of all four possible bridge site configurations tested at a coverage of 0.75 ML on the Pt(100) surface.....	37
Figure 26: Top and side view of the final geometry of configuration 4 (most stable) of the configurations tested at a coverage of 0.75 ML on the Pt(100) surface.....	38
Figure 27: Top and side views of the initial geometries of all three possible bridge site configurations tested at a coverage of 1.00 ML on the Pt(100) surface.....	38
Figure 28: Gibbs energy of adsorption at 1 atm for all three possible coverages on Pt(100) over a range of temperatures.....	40
Figure 29: Zoomed in view of the Gibbs energy of adsorption at 1 atm for all three possible coverages on Pt(100) over a range of temperatures .....	41
Figure 30: Gibbs energy of adsorption at 25 °C for all three possible coverages on Pt(100) over a range of pressures .....	41
Figure 31: Side view of the three-dimensional plot of all interacting surfaces used to develop the phase diagram for Pt(100) .....	42
Figure 32: Phase diagram for the adsorption of diatomic oxygen on Pt(100) .....	43
Figure 33: Top and side views of the initial geometries of all five possible adsorption sites tested at a coverage of 0.25 ML on the Pt(111) surface .....	45
Figure 34: Top and side views of the final geometries of all five possible adsorption sites tested at a coverage of 0.25 ML on the Pt(111) surface .....	46
Figure 35: Top and side view of the final geometry of configuration 6 (most stable geometry) at 0.50 ML on the Pt(111) surface .....	48
Figure 36: Top and side view of the final geometry of configuration 4 (most stable geometry) at 0.75 ML on the Pt(111) surface .....	49
Figure 37: Gibbs energy of adsorption at 1 atm for all three possible coverages on Pt(111) over a range of temperatures.....	51
Figure 38: Zoomed in view of the Gibbs energy of adsorption at 1 atm for all three possible coverages on Pt(111) over a range of temperatures .....	51
Figure 39: Gibbs energy of adsorption at 25 °C for all three possible coverages on Pt(111) over a range of pressures .....	52

Figure 40: Side view of the three-dimensional plot of all interacting surfaces used to develop the phase diagram for Pt(111) ..... 53  
Figure 41: Phase diagram for the adsorption of diatomic oxygen on Pt(111) ..... 53

## Nomenclature

$\sigma$	- Symmetry Number of Molecule
$c$	- Speed of Light in a Vacuum
DFT	- Density Functional Theory
EELS	- Electron Energy Loss Spectroscopy
$k_B$	- Stefan-Boltzmann Constant
fcc	- Face Centred Cubic
$g$	- Degeneracy Number of Molecule
$G_i(T, P)$	- Gibbs Energy of component $i$ at a given temperature and pressure
$h$	- Planck's Constant
hcp	- Hexagonal Close Packed
$H_i(T, P)$	- Enthalpy of component $i$ at a given temperature and pressure
$I_x$	- Moment of Inertia About the $x$ Axis
ML	- Monolayer of Coverage
MtOE	- Megatonnes of Oil Equivalent
$M_w$	- Molecular Weight
$N_A$	- Avogadro's Number
$n_{rot}$	- Rotation Number for Molecule
P	- Pressure
PBE	- Perdew–Burke–Ernzerhof Functional
Pt	- Platinum
R	- Universal Ideal Gas Constant
$S_i(T, P)$	- Entropy of component $i$ at a given temperature and pressure
T	- Temperature
VASP	- Vienna Ab initio Simulation Package
$\nu_i$	- Vibrational Frequency of Component $i$

## Glossary

- Adsorption** : The adhesion of gaseous atoms, ions or molecules to a solid surface
- Cathode** : The negatively charged electrode where the reduction half reaction of a redox reaction occurs within an electrochemical cell
- Coverage** : The number of adsorbates per adsorption surface atoms, measured in ML (monolayer)
- Density Functional Theory** : A computational quantum mechanical meddling method used to investigate the electronic structure of many bodied systems such as molecules or atoms.
- Nanoparticle** : A particle between 1 to 100 nm (nanometres) in size
- Reduction Oxidation (Redox) Reaction** : A chemical reaction involving the transfer of electrons between two species
- Supercomputer** : A computer with high level computational power when compared to a general-usage computer, implemented for particularly intensive tasks in various fields including molecular modelling.
- Vibrational Analysis** : Investigation on an atom or molecules translational and rotational movement corresponding to wavelengths
- Vienna Ab-initio Simulation Package (VASP)** : A simulation package which conducts ab initio quantum mechanical molecular dynamics through various methods with the primary function for DFT calculations based upon a given functional

# 1. Introduction

## 1.1 Background

Since 2006, the global demand for energy has increased by over 18% (British Petroleum, 2017). This increase has been met by growing production from several sources both renewable and non-renewable however, the primary contributors are still those of natural gas and oil. Consequently, there is an ever-growing need to develop forms of renewable energy as a substitute for these main contributors. An example of such a solution is fuel cell technology, which converts reagents into electrical energy via two redox reactions. The reduction redox reaction, in Pt based fuel cells, at the cathode involves the adsorption of oxygen onto platinum and has been found to be a limiting step to the overall efficiency of the fuel cell (Norskov et al., 2004). Typical  $H_2$  has been used as a reagent in fuel cell operations but due to the cost of transportation and production of  $H_2$  alternative feed gases are often desired. One such alteration is a methanol-based fuel cell which makes use of the same reduction reaction, which includes oxygen adsorption onto platinum.

In addition to its use as a fuel cell feed source, methanol is also a desirable alternative to traditional liquid fuels such as gasoline due to its high energy density. The demand for liquid fuel is exponentially increasing due to the rapid growth of the transportation industry. Methanol is traditionally produced using synthesis gas (a mixture of hydrogen and carbon monoxide); however, the production of synthesis gas is highly energy intensive as the methanol production occurs in a two-step process (Gesser, Hunter & Prakash, 1985). An alternative method of producing methanol is via the direct oxidation of methane which has substantially lower energy demands (Fratesi, Gava & Gironcoli, 2007). This reaction involves methane reacting with adsorbed oxygen on a platinum based catalyst; however, this reaction has been shown to be sensitive to the catalyst oxygen coverage, favouring higher coverages which limit side reactions. It is postulated that if full coverage of oxygen on the platinum surface can be achieved, then these side reactions can be limited and the methanol production favoured.

In both fuel cell operations and reaction systems the interactions of oxygen with the Pt surface has proved to be an important parameter to understand. However, research into oxygen interactions is often theoretically limited to O adsorption, due to the dissociative adsorption of  $O_2$  above 150 K (Gland, Sexton & Fisher, 1980). These models are often theorized at low coverages and the adsorption configurations when a catalyst approaches full saturation are often overlooked. For these reasons furthering our understanding of how  $O_2$  dissociates and at what coverages diatomic coverage becomes more stable than atomic can help to improve both fuel cell and reaction based system operations.

## 1.2 Problem Statement

A greater understanding of the geometries and adsorption energies for the adsorption of diatomic oxygen onto platinum for use in reaction based systems utilizing oxygen. Furthermore, research into the obtainable coverages and energies of this adsorption at varying temperature, and oxygen partial pressure could lead to the optimisation of operating conditions for the platinum oxidation catalyst in industry.

## 1.3 Scope of Study

This research is limited to the study of the adsorption of diatomic oxygen on the Pt(111) and Pt(100) platinum surfaces, which when combined represent an ideal Pt nanoparticle. Consequently, the study of the adsorption of atomic oxygen and intermediate surfaces will not be investigated. Furthermore, it will be assumed that the preferred adsorption site of diatomic oxygen on each surface will be the same at all coverages; therefore, a preferred adsorption site for each surface will be determined at a coverage of 0.25ML and then only this site will be investigated at higher coverages. Additionally, this study will focus on O<sub>2</sub> interactions with the Pt surface and not on the reactions within fuel cells or oxidation involving adsorbed oxygen species.

## 1.4 Objectives of Study

- Determine the most stable adsorption sites of diatomic oxygen on the Pt(111) and Pt(100) platinum surfaces and the associated adsorption energies.
- Understand the adsorption of diatomic adsorption of oxygen on the Pt(111) and Pt(100) surfaces as a function of temperature, oxygen partial pressure and coverage.
- Develop a surface phase diagram for the adsorption of diatomic oxygen on the Pt(111) and Pt(100) platinum surfaces to further the understanding of O<sub>2</sub> adsorption onto Pt.

## 1.5 Key Questions

- What are the preferred adsorption sites and the associated adsorption energies for diatomic oxygen on the Pt(111) and Pt(100) surfaces?
- Is the adsorption of diatomic oxygen on the Pt(111) and Pt(100) surfaces molecular or dissociative, and does this change at varying temperatures, oxygen partial pressures and coverages?
- How does the obtainable coverage and associated energy change as a function of temperature and oxygen partial pressure?
- At what conditions could a Pt nanoparticle be fully saturated with diatomic oxygen?

## 2. Literature Review

### 2.1 Global Energy Demand

The global demand for energy since 2006 has increased significantly, evident by the total global consumption of energy increase of 18% in MToE (Megatons of equivalent in oil) since 2005 according to British Petroleum (2017). This trend of increasing global total energy consumption per year over the past decade is illustrated in Figure 1.

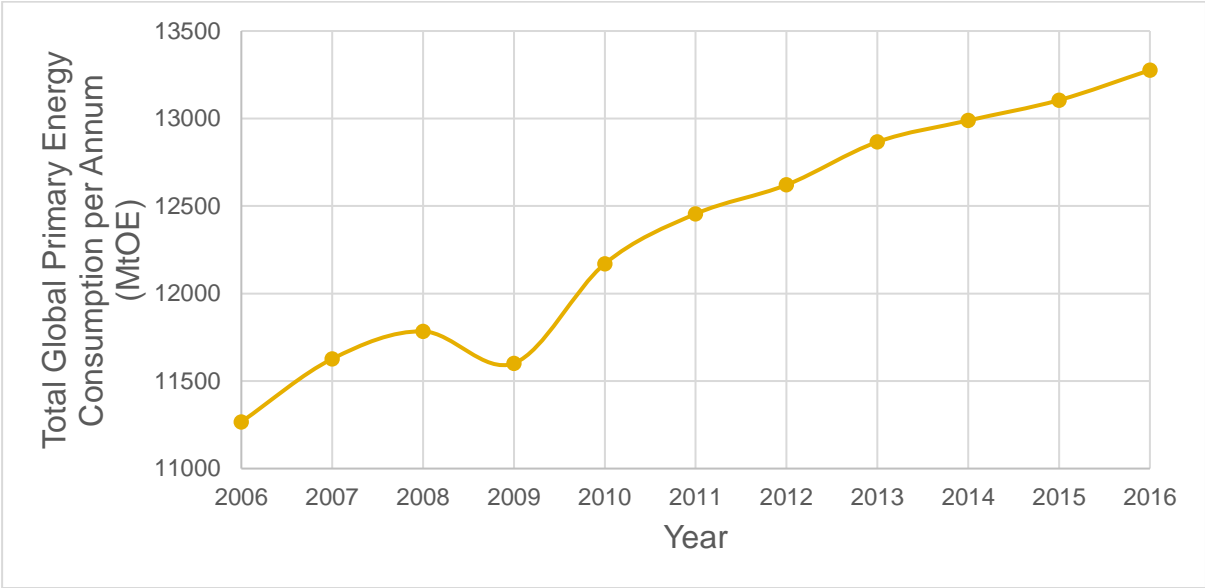


Figure 1: A plot of total global energy consumption per annum (MToE) between 2006 and 2016 (British Petroleum, 2017)

In order to match these increasing energy demands, usage of fossil fuels such as oil, coal and natural gas has accelerated; resulting in negative impacts on the environment due to the extraction methods of these fuels and the release of greenhouse gases. Furthermore, fossil fuels are finite, whereby dependence on these sources of energy creates only a temporary solution to the large and ever increasing global energy demand.

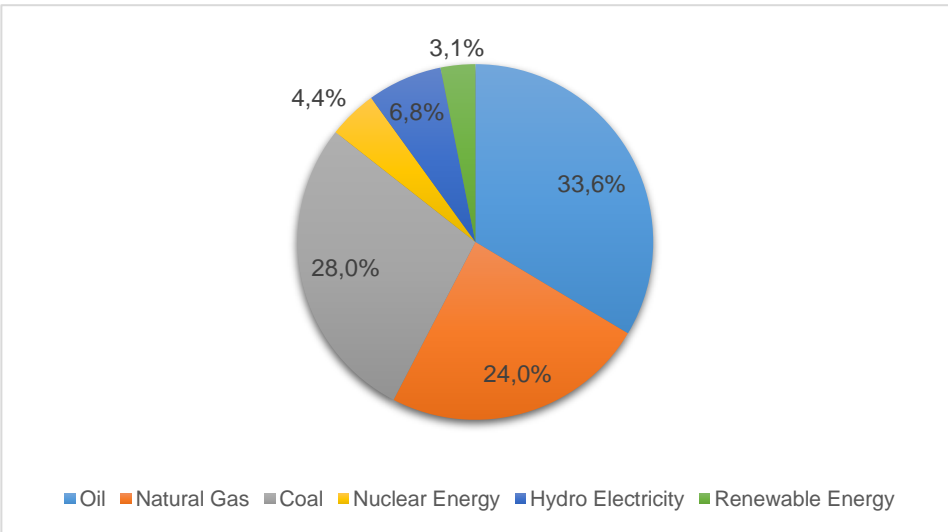


Figure 2: Breakdown of global primary energy consumption in 2016 (British Petroleum, 2017)

Increased investigation into possible renewable energy sources has served to counter the negative impact of increased fossil fuel dependence; however, renewable energy at present accounts for only 3.10% of the world's energy production according to British Petroleum (2017). A breakdown of global energy consumption by energy source for 2016 is presented in Figure 2, which serves to demonstrate the significant dependence of oil, coal and natural gas as the primary sources of global energy, all of which are classed as non-renewable energy sources.

## 2.2 Fuel Cells and Oxygen Based Reactions

The highly increasing global demand for energy, coupled with the historical energy dependence on non-renewable fossil fuels has led to an increasing need for a viable renewable energy solution. An example of a possible renewable energy resource is the fuel cell (Barbir, 2005). This energy source is highly efficient; as it maximises fuel conversion into electrical current while simultaneously minimising the production of harmful emissions (Barbir, 2005). A conventional fuel cell produces energy via a redox reaction between hydrogen and oxygen. The half-cell reactions within a conventional fuel cell are summarised below and indicate the oxidation of hydrogen occurring at the anode and the reduction of oxygen at the cathode (Barbir, 2005).



The oxygen half reaction, involving the adsorption of oxygen onto a metal surface to catalyse the reaction, is a significant limiting step to the efficiency of this process, prompting substantial research into this matter (Barbir, 2005). Further limitations to this energy solution is the requirement of hydrogen as a feed to the process – which poses safety concerns due to storage and transportation. One alternative feed to a fuel cell is methanol, which can be oxidised in the presence of water to drive the oxygen based cathode reaction (Liu et al., 2006). Direct methanation fuel cells, implement the same fundamentals as a conventional fuel cell and involve two redox half reactions occurring at the anode and cathode as presented below (Liu et al., 2017).



A clear similarity between the varying fuel cell technologies is the cathode reduction half-cell reaction, which involves the reduction of gaseous oxygen on a metal electrode surface to form water. The adsorption of oxygen onto the electrode surface is an important step to the overall fuel cell function of both, whereby the choice of electrode material is essential to the operation (Liu et al., 2006). A poor selection of electrode material may result in a fuel cell which is rate limited by the mass transfer of oxygen to the electrode surface, limiting the overall efficiency of the cell, while an optimal electrode material choice may result in more stable operating conditions and greater

fuel cell performance (Norskov et al., 2004). According to Norskov et al. (2006) platinum is the most suitable catalyst for the oxygen reduction half reaction as it provides an optimal balance between adsorption stability and proton transfer rate. Consequently, a study of the adsorption of oxygen on a platinum surface serves as a central task to enhancing fuel cell technology.

Despite the advantages in power generation posed by newly researched renewable energy sources such as fuel cells, there is limited available application within the energy intensive transportation industry, which will continue to require liquid fuels (British Petroleum, 2013). Large scale transportation of goods and services, particularly within aviation and railway industries, requires significant power generation beyond the capability of fuel cell powered motors. This, coupled with the projected 8.40% increase in liquid fuel demand from 2015 to 2030 from the current consumption of 95 million barrels of oil per day (British Petroleum, 2013), indicates that continued research into high energy density liquids will continue to show importance.

High energy density liquid fuels are fuels which are capable of releasing large amounts of energy from relatively low volumes, indicating high specific-energy. High energy density fuels are conventionally dominated by refined fossil fuels such as oil and diesel; however, a more flexible source of fuel is desired to address the limitations of these non-renewable energy sources (Reed & Lerner, 1973). One such example is methanol, which has a relatively low boiling point of 64.60 °C and a high energy density of 46.40 MJ/kg, which allows for combustion at low temperatures with a high energy output (Green & Perry, 2008).

Methanol is traditionally produced using synthesis gas, which is a mixture of hydrogen and carbon monoxide, via the following reaction:



Production of syngas is however costly and unsafe due to high operating temperatures around 800 °C (Gesser, Hunter & Prakash, 1985). Consequently, the production of methanol using the oxidation of methane, as shown below, has recently gained increased significance as a possibility to meet the global liquid fuel demand:



As proposed by Foster (1985), this reaction takes place on a platinum surface where adsorbed oxygen reacts with the methane to form methanol. However, this reaction competes with two undesired side reactions which both involve the dehydrogenation of methane, either with or without oxygen, onto the surface instead of reacting with the adsorbed oxygen (Fratesi, Gava & Gironcoli, 2007). The two undesired side reactions, where (a) represents a component adsorbed onto the platinum surface, are as follows:



These two side reactions can be limited by increasing the coverage of oxygen on the platinum surface, therefore increasing the selectivity towards methanol. Furthermore, a clearer understanding of the adsorption of oxygen onto the platinum catalyst, especially at varying coverages, will lead to an optimisation of operating conditions and increase the efficiency of similar process using adsorbed oxygen (Fratesi, Gava & Gironcoli, 2007).

The study of the adsorption of oxygen on platinum has significant importance in various industrial applications. New technologies which aim to create sustainable, renewable energy, such as fuel cells (Liu et al., 2006), depend highly on this research. Further applications of this research include the production of methanol via direct oxidation of methane (Gesser, Hunter & Prakash, 1985), with the aim of using it as a liquid fuel alternative to gasoline/diesel. Consequently, a better understanding of the adsorption energies and preferred geometries associated with the adsorption of oxygen on platinum could lead to significant advancements in creating a more sustainable energy production.

### 2.3 Platinum Nanoparticles and Surfaces

In order to accurately model a platinum surface, a clear understanding of all possible geometries of platinum in a lattice must be highlighted and the most stable configuration established. A platinum surface consists of a lattice containing platinum nanoparticles on which adsorption can occur (Tripkovic et al., 2014). The overall geometry of any metal nanoparticle is determined on the basis of minimising the surface free energy in the system.

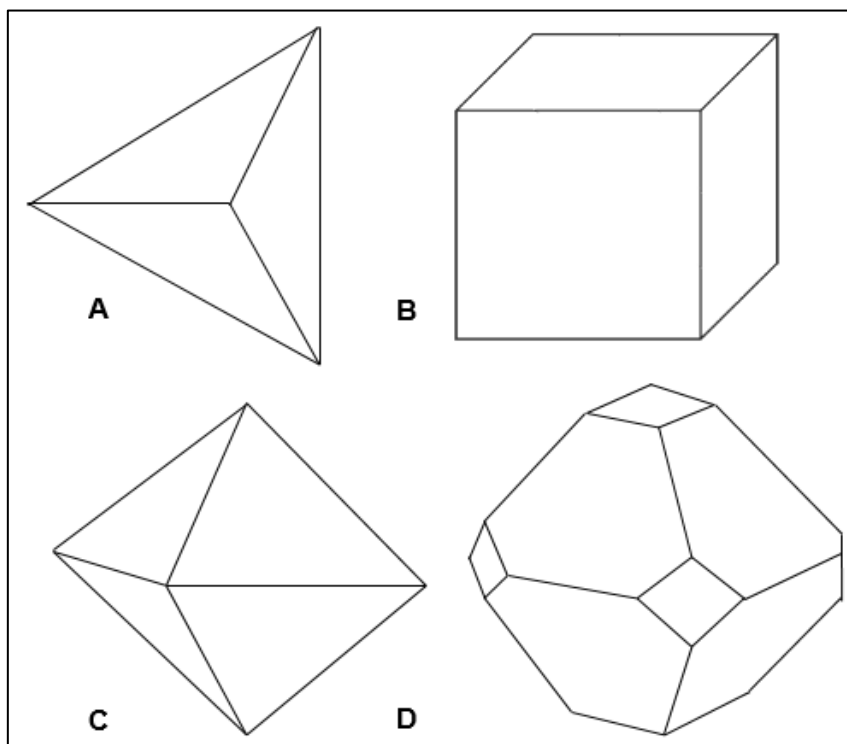


Figure 3: Nanoparticle shape configurations: A-Tetrahedron, B-Cubic, C-Octahedron, D-Truncated Octahedron

According to Tripkovic et al. (2014), four equilibrium shapes are found to represent the overall geometry of metal nanocrystals as highlighted in Figure 3; they are: tetrahedron (A), cubic (B), octahedron (C) and truncated octahedron (D).

Therefore, any metal nanoparticle will exist as one of these four geometries. However, a specific geometry will dominate based on the one which creates the surface planes that minimise the free surface energy of the system. According to Tripkovic et al. (2014), a truncated octahedron nanoparticle is the most thermodynamically stable for a platinum nanoparticle. The truncated octahedron consists of two different surfaces on which molecules or atoms can adsorb, namely: the Pt(111) and Pt(100) surfaces (Tripkovic et al., 2014), highlighted in Figure 4.

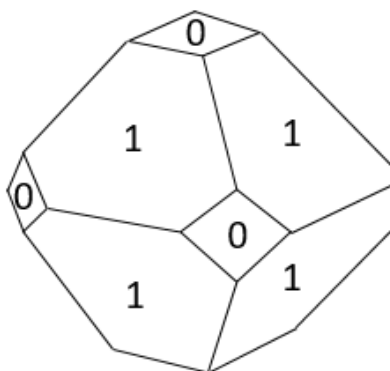


Figure 4: Dominant surfaces on a platinum truncated tetrahedron nanoparticle (1-Pt(111),0-Pt(100))

These surfaces contain various arrangements of platinum atoms within the lattice, impacting the surface and lower layer geometries and the available sites for adsorption. The Pt(111) surface refers to a surface which intersects the fcc unit cell in the 111 plane. Pt(111) arranges platinum atoms such that the second layer of atoms follows hexagonal cubic packing (hcp) while the third layer is arranged in face centred cubic packing. This arrangement of layers repeats every three layers down and is unique to a 111 cut of a fcc unit cell. The Pt (111) lattice arrangement is visualised in Figure 5 and results in four available adsorption sites at the surface, namely: the fcc hollow site which occurs where there is a gap in the second layer platinum arrangement, the hcp site which occurs directly above a second layer platinum atom, a bridge site which occurs between two platinum surface atoms and a top site which occurs above a platinum surface atom (Lynch & Hu, 2000).

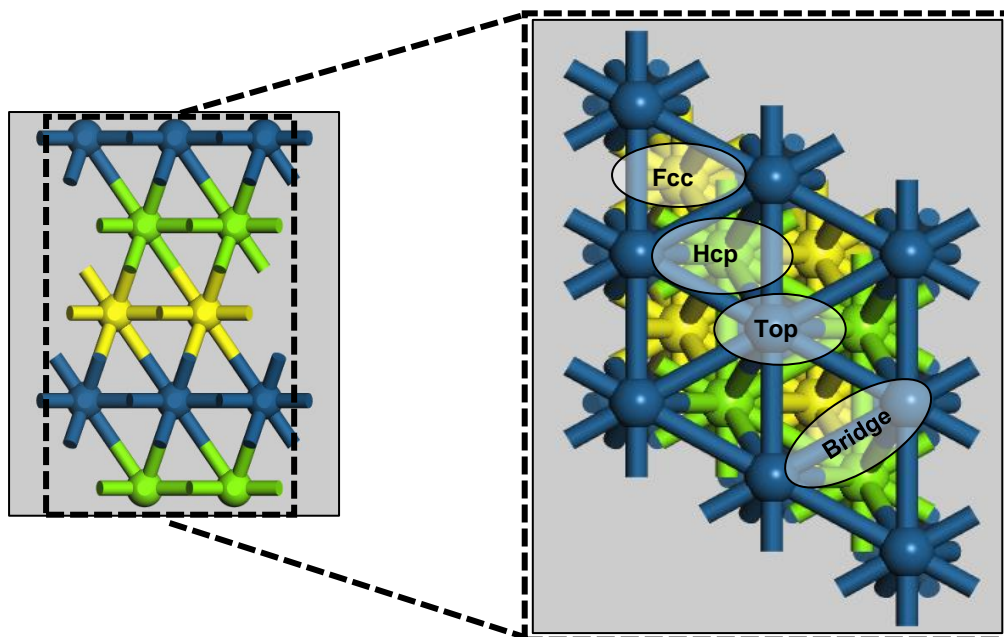


Figure 5: Side and top views of a Pt(111) surface showing all possible adsorption sites

The Pt(100) surface, visualised in Figure 6 arranges platinum atoms in a fcc packing arrangement which repeats every two layers. This surface has three available adsorption sites consisting of the hcp, bridge and top sites (Gu & Balbuena, 2007).

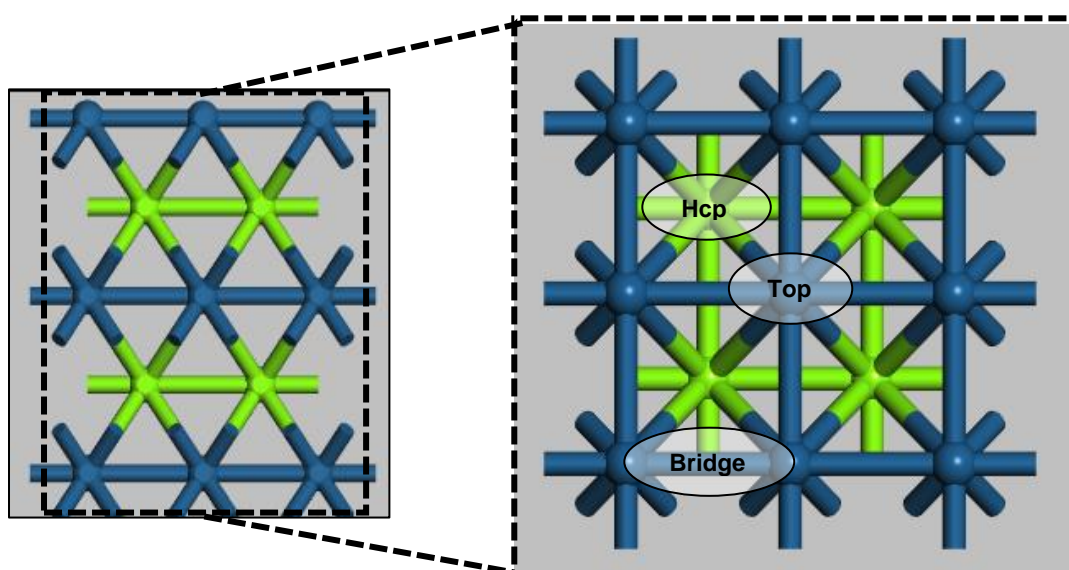


Figure 6: Side and top views of a Pt(100) surface showing all possible adsorption sites

## 2.4 Studies on Oxygen Adsorption to Platinum

In order to understand the adsorption of oxygen onto platinum, it is vital to investigate the preferred adsorption sites of oxygen on both the Pt(111) and Pt(100) to ensure that the thermodynamically preferred adsorptions are being represented. Furthermore, energies will be dependent on coverage, temperature and oxygen partial pressure of the system. A possible method for determining this information is to perform a Density

Functional Theory (DFT) study (Karp et al., 2012). A DFT calculation minimises the total energy in a system and delivers the most thermodynamically stable geometry of the system along with its associated total energy. This study would be able to effectively provide the preferred method and sites for adsorption of oxygen on platinum at varying conditions by iterating the total energy in the system until it reaches a preferred convergence criteria. DFT does this by solving Schrodinger's equation, which represents the possible energy levels of a molecular system in the form of a wavefunction and the probability of finding an electron in a particular position in space (Car & Parrinello, 1985). Effectively, DFT solves for the total energy of a system by minimising the energy of the wave function based on electron densities (Car & Parrinello, 1985).

Other methods used to understand the adsorption of oxygen on platinum are often limited. Multiple studies have been carried out using various spectroscopy and microscopy methods such as Gland, Sexton & Fisher (1980) who use Electron Loss Spectroscopy (EELS), Ultraviolet Photoemission and Thermal Desorption. However, these methods are limited to finding the preferred site and nature of adsorption, and an accurate measurement of the binding energy cannot be obtained. Single-crystal adsorption calorimetry can be used to calculate the adsorption energy (Fiorin, Borthwick & King); however, it is suggested by Karp et al. (2012) that this method is not accurate at coverages higher than 0.15 ML.

When oxygen adsorbs onto platinum, it can either adsorb as diatomic oxygen to a single site or dissociate into two atomic oxygens, adsorbing as a single atom. It is suggested by Gland, Sexton & Fisher (1980) that this depends highly on both temperature and coverage. Ford, Xu & Mavrikakis (2005) performed a DFT study on the adsorption of atomic oxygen on Pt(111). They found that oxygen preferred to adsorb onto the fcc hollow site at a coverage of 0.25 ML. This coverage indicates that one oxygen atom is adsorbed per every four platinum atoms on the surface. Ford, Xu & Mavrikakis (2005) further mention that this coverage of 0.25 ML represents the saturation coverage of the system at room temperature.

The adsorption energy on the fcc site was found to be -3.87 eV, while the O-Pt bind energy for the top and hcp sites were -2.46 eV and -3.43 eV respectively and the bridge site was determined to be unstable (Ford, Xu & Mavrikakis, 2005). Consequently, the fcc site was found to be the most stable given the low adsorption energy. Furthermore, this study confirmed the accuracy of the DFT calculations by comparing the theoretically computed adsorption energy of -3.87 eV to the experimental value of -3.7 eV (Ford, Xu & Mavrikakis, 2005). The work done by Ford, Xu & Mavrikakis (2005) is however limited to only Pt(111) at room temperature with no investigation on adsorption of atomic oxygen at increasing coverages. This work may be improved upon through the addition of adsorption energies of atomic and diatomic oxygen on both Pt(111) and Pt(100) at varying temperatures and coverages to better understand adsorption of oxygen on platinum.

A similar study, conducted by Lynch & Hu (2000), investigated DFT calculations for atomic oxygen on Pt(111). This study concluded that the fcc adsorption site was the most thermodynamically stable, with an associated adsorption energy of -4.26 eV at a coverage of 0.25 ML. They found that, following the stable fcc site, the hcp hollow site was the second most stable adsorption site with an energy of -3.79 eV; while the bridge and top sites had binding energies of -3.63 eV and -2.63 eV respectively. This indicates that the top site is very unstable and it is highly unlikely to find adsorption occurring there. This study agrees with the work conducted by Ford, Xu & Mavrikakis (2005) when stating the most stable adsorption site at a 0.25 ML coverage. Large differences in adsorption energies at the various adsorption sites are present when comparing the works of Ford, Xu & Mavrikakis (2005) with Lynch & Hu (2000), as can be seen in Table 1 which summarises the adsorption energy results of both studies.

Table 1: Comparison between calculated adsorption energies in the studies carried out by Ford, Xu & Mavrikakis (2005) and Lynch & Hu (2000) on the atomic adsorption of oxygen on Pt(111)

	Ford, Xu & Mavrikakis (2005)	Lynch & Hu (2000)
atop	-2.46 eV	-2.63 eV
bridge	Unstable	unstable
fcc	-3.87 eV	-4.26 eV
hcp	-3.43 eV	-3.79 eV

These differences in reported adsorption energies may be due to the differences in calculation methods implemented by the two groups. Ford, Xu & Mavrikakis (2005) implemented the Kohn-Sham Hamiltonian to determine the electron density while implementing the GGA-PW91 functional, while Lynch & Hu (2000) implemented the Hellmann-Feynmann theorem to calculate forces on atoms. Given that the experimental value of -3.70 eV was determined through the work of Ford, Xu & Mavrikakis (2005), the theoretical adsorption energy of -3.87 eV determined from this study presents a more accurate value to experimental data, indicating this study method may be more reliable. As was also the case in Ford, Xu & Mavrikakis (2005), the Lynch & Hu (2000) study only investigates the adsorption at a coverage of 0.25 ML. This is very limited as the adsorption energies and preferred sites may differ when the coverage is changed.

Fiorin, Borthwick & King (2009) studied the adsorption of diatomic oxygen on Pt(111) at varying coverages at 300K. This study used the single-crystal adsorption calorimetry method (SCAC) to calculate adsorption energies by making use of a thin film to measure temperature changes in the order of 0.10 K. At a coverage of 0.25 ML, they calculated the energy of adsorption to be -1.30 eV (Fiorin, Borthwick & King, 2009). This is significantly different to the experimental value of -3.70 eV, indicating very inaccurate measurements. Furthermore, Karp et al. (2012) directly opposes the work presented by Fiorin, Borthwick & King (2009) as they suggest that an incorrect optical reflectivity was used for Pt(111) which led to a 40% error in the adsorption energies

calculated. Additionally, Karp et al. suggests that calorimetry in general does not measure binding energies accurately above a coverage of 0.15 ML due to low sticking probabilities of oxygen at these coverages. Consequently, Karp et al. (2012) recalculated the adsorption energies presented in Fiorin, Borthwick & King (2009) using a DFT study in order to model the adsorption more accurately. This research calculated the binding energy of oxygen on platinum to be -3.60 eV, while the adsorption was found to be dissociative at a coverage of 0.25 ML. The presented DFT results indicates similar adsorption energies to that of the experimental data gathered in the work by Ford, Xu & Mavrikakis (2005) of -3.70 eV, indicating accurate results. Karp et al. (2012) indicates that DFT calculations are more reliable when determining adsorption energies when compared to SCAC methods. The adsorption energy presented by Karp et al. (2012) is very similar to Ford, Xu & Mavrikakis (2005), while it is reasonably close that calculated by Lynch & Hu (2000). These values differ as Karp et al. (2012) makes use of the RPBE functional in their DFT calculations, which differs from the other studies.

Limited information on adsorption energies of oxygen on Pt(100) is available due to this surface forming a small fraction of the overall platinum nanoparticle surface area (Tripkovic et al., 2014). Research conducted by Gu & Balbuena (2007) implementing DFT calculations on atomic oxygen adsorption on a Pt (100) surface demonstrated that, at a coverage of 0.25 ML and ambient temperature, the preferred adsorption site was the bridge site. The corresponding adsorption energy at the bridge site at this coverage was calculated to be -4.62 eV, while the top and hcp sites had binding energies of -3.56 eV and -4.31 eV respectively (Gu & Balbuena, 2007). This study was part of the limited available information on adsorption of oxygen on Pt(100) obtained from a DFT study implementing the PBE functional. Additional research into the adsorption of oxygen on Pt(100) must be carried out to better understand this system, especially at varying coverages and temperatures.

In addition to the adsorption energies, a clear understanding of the nature and geometry associated with the adsorption of oxygen on platinum is also required. Furthermore, the energies and preferred adsorption sites presented thus far are only applicable at specific temperatures and coverages. Gland, Sexton & Fisher (1980) suggest that the adsorption of diatomic oxygen dominates at temperatures below 120 K, while the adsorption is dissociative (atomic oxygen adsorbs on the platinum surface) between 150 K and 1000 K. Additionally, at temperatures higher than 1000 K, subsurface oxide is formed. Gland, Sexton & Fisher (1980) produced these findings by using EELS, which can identify the type of adsorbate present on the surface based on measured vibrational frequencies. This study is useful in understanding the effect of temperature on the nature of adsorption and can be used to understand possible reaction conditions; however, it is very limited in demonstrating the effect of coverage on the adsorption, while no adsorption energies are presented.

Work conducted by Puglia et al. (1995) demonstrates that at low temperatures, below 25 K, oxygen physisorbs to a platinum surface, while at temperatures between 25 K

and 150 K diatomic chemisorption to the surface occurs. Furthermore, at temperatures above 150 K, atomic adsorption of oxygen dominates (Puglia et al., 1995). This study serves to reinforce the results obtained from Gland, Sexton & Fisher (1980) by indicating similar temperature ranges for diatomic and atomic (dissociative) adsorption on Pt (111) surfaces. Additionally, they indicate that a saturation coverage of 0.25 ML, presenting a similar result to that reported in Ford, Xu & Mavrikakis (2005). Various spectroscopic methods were used to identify the surface adsorbate in Puglia et al. (1995) and is therefore limited to the identification of the adsorbate without presenting associated adsorption energies.

Both Karp et al. (2012) and Gu & Balbuena (2007) propose that increasing the coverage of oxygen will decrease the adsorption energy, leading to a decrease in the stability of the system. However, none of the research mentions any change in the nature of adsorption when coverage is increased.

In conclusion, DFT studies provide vital information about an adsorption system and can aid development of industrial catalysts. There is substantial research already in the field of oxygen adsorption onto platinum; however, there is a clear gap in the knowledge with regards to adsorption onto the Pt(100) surface, while limited studies significantly explore the effect of varying temperature and coverage on the system.

### 3. Experimental Method

#### 3.1 Methodology Overview

The adsorption of diatomic oxygen on Pt(111) and Pt(100) will be calculated using a theoretical DFT study. Each simulation will be run using *VASP* in order to determine the total energy of the system at 0 K. This programme will aim to minimise the energy in a system which will be created using the visualisation software *Material Studios*. The *VASP* will run on a cluster of supercomputers which allow the simulation to perform DFT calculations and iterate the total energy of the system, by moving a set number of atoms and altering the geometry of the system, until a convergence criteria of 10 meV.Å<sup>-1</sup> is met. These calculations will be done using a GGA-PBE functional as this functional reasonably approximates metal adsorbate interactions (Xu & Goddard, 2004). The total energy of the system can then be used in conjunction with the final geometry of the system to draw conclusions about the geometry and energy of adsorption. Furthermore, a vibrational analysis will be carried out using *VASP* in order to adjust the results to various temperatures and pressures using the appropriate thermodynamic models.

#### 3.2 Calculation of Adsorption Energy

The DFT calculations performed by *VASP* returns the total energy of each simulated system. DFT calculations are performed at 0 K, and as such the calculated total energy is equivalent to the Gibbs free energy of the system. It is of interest for this study to determine the Gibbs energy of adsorption of diatomic oxygen on various sites on both the Pt(111) and Pt(100) surface. Therefore, in addition to the total energy of an adsorbed system at 0 K, both the total energies of the same clean platinum surface and a plain diatomic oxygen molecule at 0 K must be found in order to calculate adsorption energy. The equation used in this study to calculate adsorption energy is depicted graphically in Figure 7.

$$G_{adsorption}(T, P) = G_{adsorbed\ slab}(T, P) - G_{clean\ slab}(T, P) - G_{O_2}(T, P) \quad (9)$$

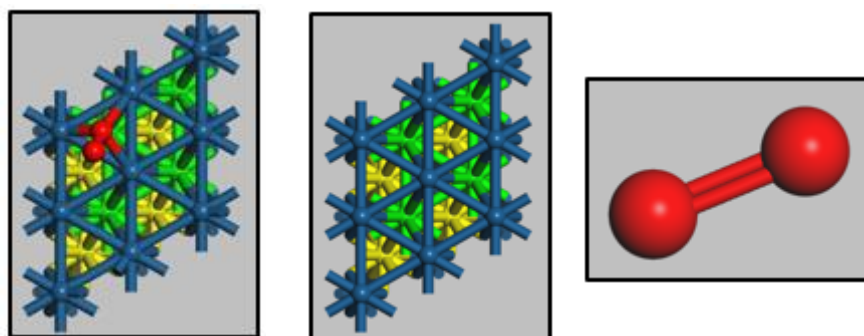


Figure 7: The method for calculating the Gibbs adsorption energy using an example of diatomic oxygen adsorbed onto a hcp site on Pt(111)

### 3.3 Modelling Oxygen

As highlighted in Figure 7, in order to calculate the Gibbs Free Energy of adsorption, the electronic energy of a pure diatomic oxygen is required. This was achieved by placing diatomic oxygen in the centre of a 10 Å x 11 Å x 12 Å box and calculating the energy using *VASP*, implementing a 1x1x1 k-point grid with a cut-off energy of 400 eV. It was found that the total electronic energy at 0 K was -9.85 eV, with a bond length of 1.23 Å. This calculated bond length was validated against the typical bond length of diatomic oxygen measured at 1.21 Å from Gray (1994). A vibrational analysis was also carried out on the system in order to obtain the vibrational frequencies required to upscale this energy into a Gibbs free energy using the thermodynamic correlations shown in Section 3.10. The vibrational analysis yielded a primary real vibrational frequency for pure diatomic oxygen of 1 565 cm<sup>-1</sup>. This analysis presented similar vibrational frequencies to that of experimental vibrational frequencies obtained from Memorial University (2017) at 1629 cm<sup>-1</sup>. Through validation against appropriate literature and experimental data, the modelling of diatomic oxygen was achieved at sufficient accuracy and models a real gas O<sub>2</sub> molecule well.

### 3.4 Model Optimisation Overview

In order to model adsorption of diatomic oxygen, the metal surface plane would need to extend infinitely in all directions to represent the atomic scale and relative lattice bulk. However, a simplified metal surface model may be used to accurately simulate the system within reasonable convergence. A simplified model of a metal surface would involve finite dimensions, whereby DFT calculations performed on this model would yield accurate results within a chosen convergence to that of bulk surface. A simplified metal surface model therefore allows for sufficiently accurate results with the benefit of creating a finite system which is easily visualised.

Computational time must additionally be considered as it serves as a significant variable and limitation within DFT studies due to the complexity of the calculations performed. Computational time may vary significantly based on the size of the model, whereby investigation into the creation of an optimised model which serves to achieve desired accuracy must consider computational time as an additional variable. Thus, a trade-off between convergence and computational time need to be considered, promoting the creation of an optimised simplified model for each platinum surface.

Selection of the dimensions of the simplified platinum surface within this study influences the number of available sites for adsorption and thus the total number of varying coverages investigated. Based on time constraints within this study, a 2x2 platinum surface was selected for the modelled Pt(100) and Pt(111) surfaces. This dimension allows for computation of multiple coverages at 0.25 ML, 0.50 ML, 0.75 ML and 1.00 ML for each surface and thus allows for a good range of coverages to be tested within a reasonable scope.

In order to create an optimised model, various parameters for the platinum surface must be considered. These parameters include the lattice parameter, k-points, cut-off energy, number of layers, number of relaxed layers and vacuum spacing where each parameter will be discussed within this paper. These parameters influence the accuracy of the model as each parameter significantly impacts the calculations performed on the system.

During the optimisation process each parameter was compared to an overestimated value, based on previous studies, as considered convergence references. The chosen overestimated values for all the parameters will be discussed in this paper and justified as the convergence references. The Gibbs adsorption energy of diatomic oxygen at 0.25 ML onto the platinum surface was then used to determine when each parameter reached convergence by comparing the adsorption to 0.25 ML adsorption at the converged reference. Differences in Gibbs adsorption energy to the reference may be investigated, where a convergence of 20 meV has been chosen for this study. This may be investigated for all parameters, where parameter values which obtain adsorption energies within the specified convergence are considered sufficiently accurate. Consideration of computational time will also be considered during this optimisation process, whereby optimal parameters will be chosen based on achieving sufficient accuracy at minimum computational time.

### 3.5 Lattice Parameter

The first variable that must be determined is the lattice parameter, as it represents the bulk Pt-Pt distance and is thus significant to both Pt(100) and Pt(111) surfaces. The lattice parameter is effectively the distance between the platinum atoms in the face-centred cubic unit cell- see Figure 8. According to experimental results (Hermann, 2011), the lattice parameter of Pt is 3.92 Å.

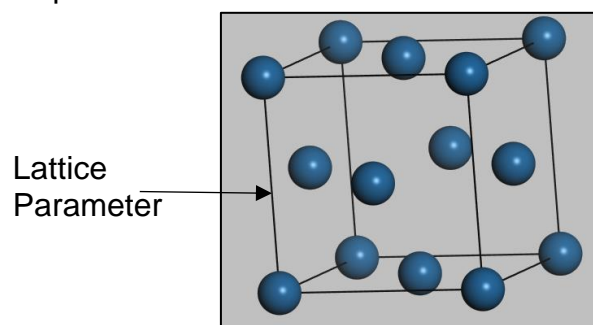


Figure 8: A face-centred Pt unit cell highlighting the lattice parameter:

The total energy of this unit cell system was calculated across a range of lattice parameters between 3.9 Å and 4.1 Å in intervals of 0.02 Å. The total energy was plotted against the lattice parameter range and fitted against a polynomial of degree 4. This polynomial was effective in predicting the acquired data with a determined  $R^2$  value of 1. The plotted data can be seen by Figure 9, which shows the total system energy for all calculated lattice parameters and indicates that the system energy reaches a

minimum and therefore has a corresponding most thermodynamically stable lattice parameter. Calculation of this minimum through differentiation of the polynomial and equating to 0 determined a lattice parameter of 3.981 Å, which will be used for the surface model. It must be noted that this calculated lattice parameter differs slightly from literature; which is due to the PBE functional overestimating bond lengths within the system (Xu & Goddard, 2004).

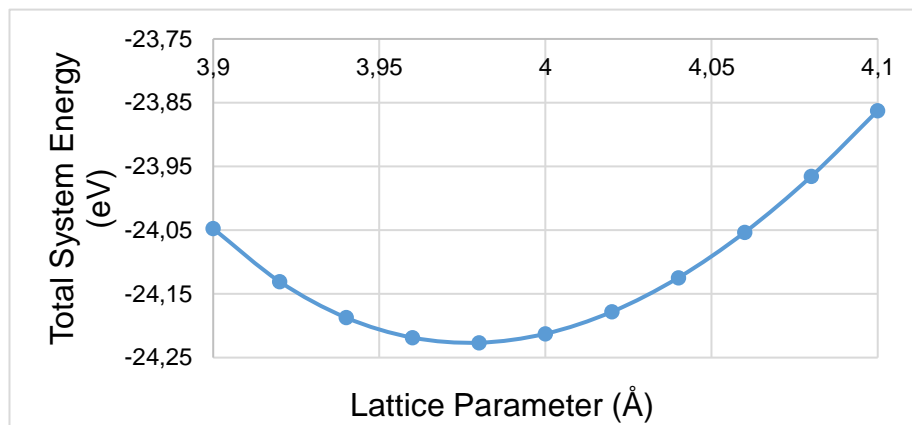


Figure 9: The total system energy versus lattice parameter for a Pt unit cell

## 3.6 Parameter Optimisation Pt(100)

### 3.6.1 Pt(100) K-Points

In order to solve infinitely extended integrals in the real space, such as those present within DFT calculations, finitely extended integrals in the reciprocal space are created. The K-point mesh is a set of points which defines space within the Brillouin zone, a reciprocal space used for solving integrals according to Bloch's theorem. The K-point sampling was optimised for the system using a conventional unit cell for bulk platinum with a lattice parameter of 3.981 Å. The investigated unit cell was set with a cut-off energy of 400 eV and vacuum spacing of 14 Å to ensure a sufficient basis for convergence. The investigated system was a 5-layered platinum slab with 2 relaxed layers, where adsorption of diatomic oxygen at 0.25 ML was implemented. Measurements of the total energy of the system at varying irreducible k-points was implemented. A reference of a 20x20x1 k-point grid for sufficient convergence was chosen, whereby energy difference to the reference of the measured bulk platinum as a function of the k-point grid was plotted. Based on the chosen convergence of 20 meV, data from Figure 10 indicates that a number of 52 irreducible k-points, representing a 10x10x1 k-point grid serves as optimal for the studied system.

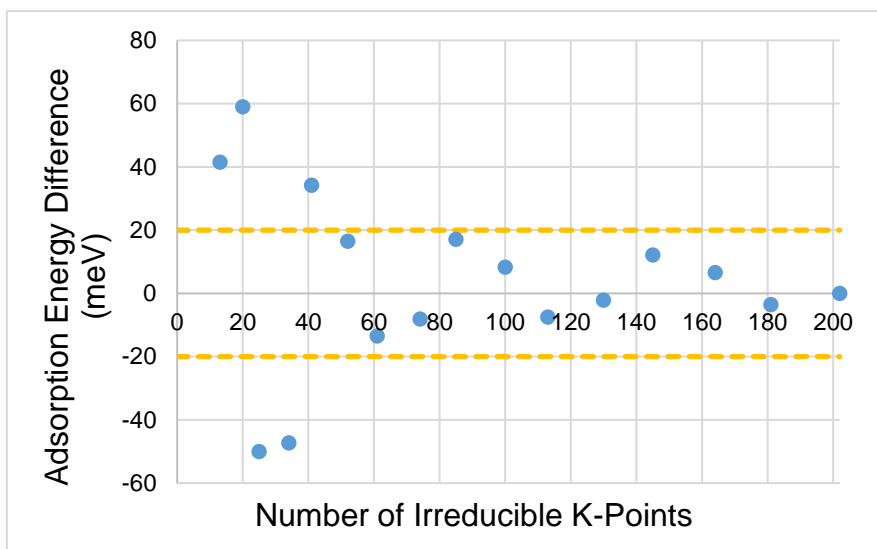


Figure 10: Adsorption energy difference versus number of Irreducible K-Points for Pt(100), measured from diatomic oxygen adsorption at 0.25ML on a 2x2 Pt surface with a vacuum spacing of 14 Å with 5 layers, 2 relaxed and a cut-off energy of 400 eV. Reference of 20x20x1 k-point grid

### 3.6.2 Pt(100) Cut-Off Energy

The cut-off energy represents the maximal energy to be considered within a DFT calculation corresponding to maximal wavelengths within the system. Cut-off energy optimisation for the system was conducted through investigation using a conventional unit cell for bulk platinum with a lattice parameter of 3.981 Å. The investigated unit cell was set with a k-point grid of 10x10x1 to ensure that a sufficient number of irreducible k-points were available, as well as a vacuum spacing of 14 Å to allow for a sufficient basis for convergence. The investigated system was a 5-layered platinum slab with 2 relaxed layers, where adsorption of diatomic oxygen at 0.25 ML was implemented. Measurements of the total energy of the system at varying cut-off energies was implemented. A reference cut-off energy of a 500 eV for sufficient convergence was chosen, whereby energy difference to the reference of the measured bulk platinum as a function of cut-off energy was plotted. Based on the chosen convergence of 20 meV, data from Figure 11 indicates that a cut-off energy of 400 eV serves as optimal for the studied system.

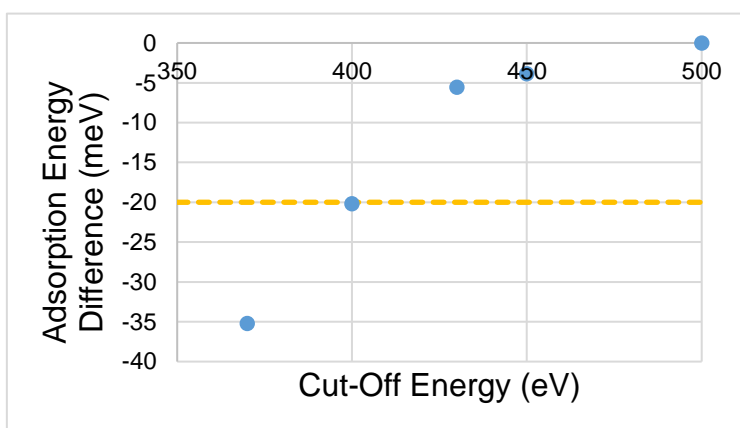


Figure 11: Adsorption Energy Difference Versus Cut-Off Energy for Pt(100), measured from diatomic oxygen adsorption at 0.25ML on a 2x2 Pt surface with a vacuum spacing of 14 Å with 6 layers, 2 relaxed and a k-point grid of 10x10x1. Reference of 500eV

### 3.6.3 Pt(100) Number of Layers

The Pt(100) surface is created by cutting the Pt unit cell in the 100 plane. Subsequently, the platinum surface is replicated in a series of layers to accurately model the system. A theoretical infinite number of layers would serve to ideally represent the atomic scale of the adsorbate to the bulk platinum lattice. The number of layers influences the electron density and thus the energy of adsorption. An infinite number of layers however does not influence the accuracy of the model within reasonable convergence, whereby an optimal number of layers may be chosen which models the system with sufficient accuracy. Previous studies have utilised 4-6 Pt layer slabs (Karp et al., 2012). Thus, a 12-layer slab was considered converged and taken as a reference with an overestimated number of layers. A number of layers corresponding to an adsorption energy difference to this reference within 20 meV was chosen as sufficiently accurate and optimal. A further consideration is computational time, as increasing the number of layers significantly influences the overall computational time for the DFT calculations with negligible influence on the accuracy of the model.

The adsorption energy was calculated for Pt(100) at 0.25 ML for all number of layers between 3 and 12; using a cut-off energy of 400 eV, a k-point grid of 10x10x1, a vacuum spacing of 14 Å and 2 relaxed layers. As can be seen in Figure 12, which represents the adsorption energy difference versus number of layers for a Pt(100) surface, the number of layers converges to the desired energy difference of 20meV when 6 layers are used to create the Pt slab. Computational time indicates steady increase as the number of layers increase, whereby 6 layers is able to obtain desired accuracy at minimum computational time.

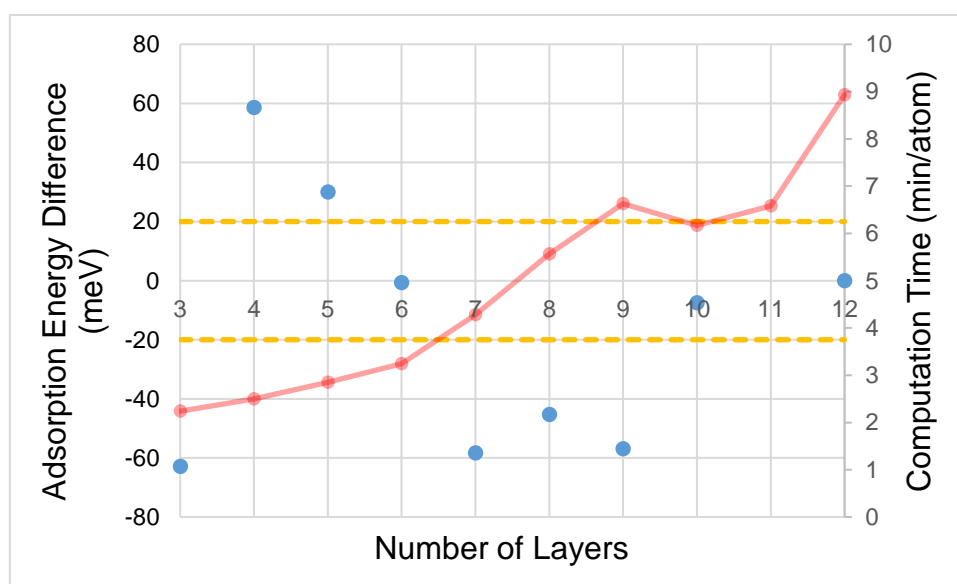


Figure 12: Adsorption energy difference versus number of layers (BLUE) for Pt(100), measured from diatomic oxygen adsorption at 0.25ML on a 2x2 Pt surface with a vacuum spacing of 14 Å with 2 relaxed layers. K-point grid of 10x10x1 and cut-off energy of 400 eV. Reference at a 12-layered slab. Computational Time against number of layers additionally plotted (RED)

### 3.6.4 Pt(100) Number of Relaxed Layers

When *VASP* runs DFT calculations on a given system, iterative calculations on the energy of the system are performed by altering the geometries of the system until a convergence is reached. When a simulation is created in *Material Studios*, a certain number of layers on the Pt slab is set to be relaxed, and therefore able to move and have varying arrangements during calculations. Although a true system would allow for movement and vibration of all atoms, this will not increase the accuracy of the model beyond reasonable convergence. Movement of atoms within lattice layers beyond a certain point will be negligible influenced by interactions on the surface. A further variable to consider is computational time, whereby allowing increased number of relaxed layers allows for significant increase in available geometries and thus increased computational time at negligible accuracy improvements. Thus, an optimal number of relaxed layers may be calculated for the selected 6-layer slab. An optimal number of relaxed layers would present adsorption energies within 20 meV to that of 5 relaxed layers, indicating sufficient convergence.

Adsorption energy was investigated through adsorption of diatomic oxygen on Pt(100) at 0.25 ML. This system implemented a cut-off energy of 400 eV, a k-point grid of 10x10x1 and a vacuum spacing of 14 Å. Adsorption energy difference against a system with 5 relaxed layers is plotted against the number of relaxed layers for Pt(100) in Figure 13, where based upon the chosen convergence of 20 meV, 2 relaxed layers has been chosen as optimal for the surface to achieve minimal computational time at the desired accuracy.

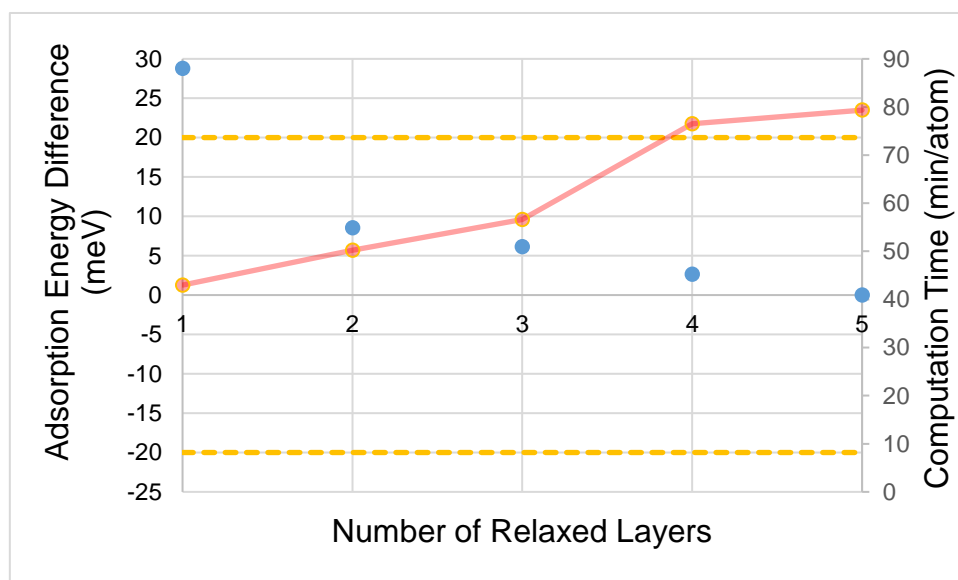


Figure 13: Adsorption energy differences against the number of relaxed layers (BLUE) in Pt(100), measured from diatomic oxygen adsorption at 0.25 ML on a 2x2 Pt surface with a 14 Å vacuum spacing, k-point grid of 10x10x1 with 6 layers and a cut-off energy of 400 eV. Reference at a 5-relaxed layered slab. Computational Time against number of layers additionally plotted (RED)

### 3.6.5 Pt(100) Vacuum Spacing

A simplified platinum surface with an oxygen adsorbate serves to represent an infinitely repeated system in the x, y and z direction. When modelling the system, selection of the vacuum space above the platinum surface is conducted, marking the distance in the x direction between the infinitely repeated surfaces as seen in Figure 14.

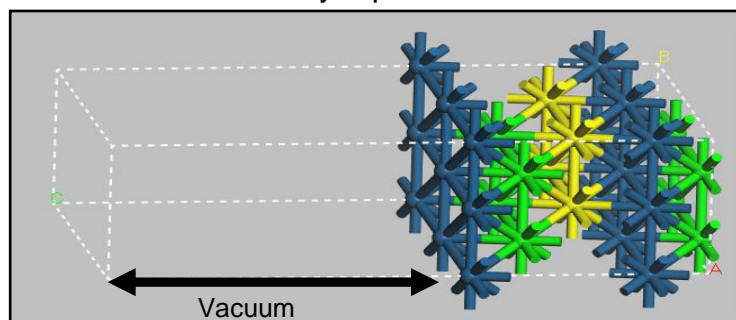


Figure 14: A Pt(111) Surface of 6 Layers with Vacuum Spacing Included

A true system would have an infinite vacuum space above the surface with no repeated surfaces in the x direction. Furthermore, proximity of a repeated surface in the x direction may result in electronic interactions with the studied system, influencing the reported adsorption energies and thus the accuracy of the model. Infinite vacuum spacing is however not required for sufficient accuracy, as increasing the vacuum spacing point an optimal length would have negligible influence of the accuracy of the model within a reasonable convergence. A further consideration is computation time, as increased vacuum spacing has a significant influence of the volume of the system and thus the computational time required to perform DFT calculations at negligible influence in accuracy. Thus an optimal vacuum spacing distance may be chosen.

Vacuum spacing of  $14\text{\AA}$  was chosen as the reference for this study, as it was assumed that this spacing would overestimate the accuracy of the system based on similar studies conducted (Karp et al., 2012). Adsorption of diatomic oxygen on a Pt(100) surface with 5 layers, 2 relaxed, at 0.25 ML was investigated with a k-point grid of  $10 \times 10 \times 1$  and cut-off energy of 400 eV. Adsorption energy difference against a  $14\text{\AA}$  vacuum spaced unit was plotted against various vacuum spacings ranging from 10- $14\text{\AA}$  for Pt(100) and is presented in Figure 15. It must be noted that a considerably high adsorption difference 16.1 meV for  $13\text{\AA}$  vacuum spacing on Pt(100) was recorded, and as such this recording has been excluded from the plot. Based on the convergence of 20 meV, all adsorption energy differences are within the desired convergence. In order to ensure consisting optimised parameter choices for both surfaces, a vacuum spacing of  $11\text{\AA}$  was chosen to optimise the Pt(100) surface based upon Pt(111) vacuum spacing optimisation discussed in this study.

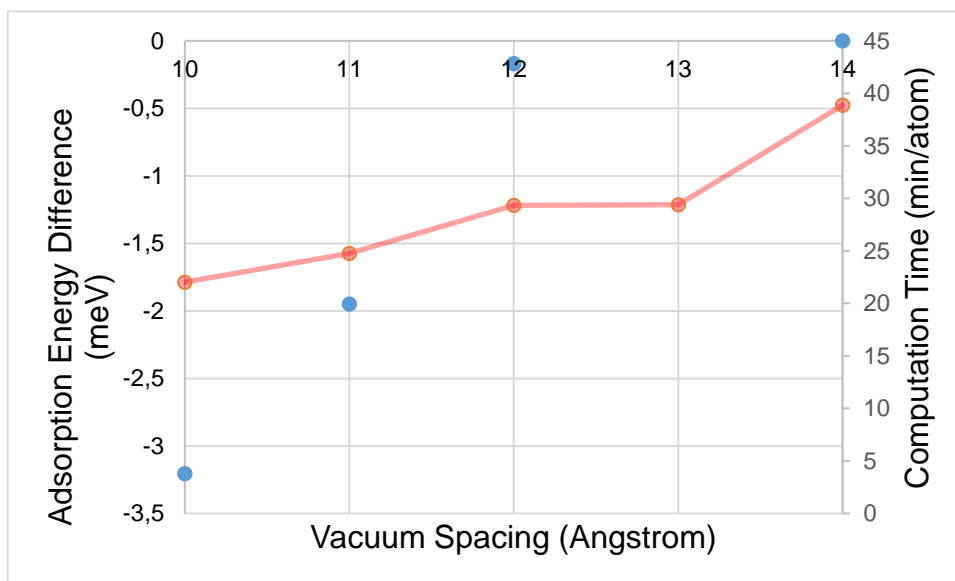


Figure 15: Adsorption Energy Difference versus Vacuum Spacing (BLUE) for Pt(100), measured from diatomic oxygen adsorption at 0.25ML on a 2x2 Pt surface with a cut-off energy of 400 eV and a k-point grid of 10x10x1, with 5 layers, 2 relaxed. Reference at a 14 Å slab. Computational Time against number of layers additionally plotted (RED)

## 3.7 Parameter Optimisation Pt(111)

### 3.7.1 Pt(111) K-Points

The K-point sampling for Pt(111) was optimised in a similar manner to that of Pt(100), using a conventional unit cell for bulk platinum with a lattice parameter of 3.981 Å. The investigated unit cell was set with the same cut-off energy of 400 eV and vacuum spacing of 14 Å to ensure a sufficient basis for convergence. The investigated system was a 5-layered platinum slab with 2 relaxed layers, where adsorption of diatomic oxygen at 0.25 ML was implemented. Measurements of the total energy of the system at varying irreducible k-points was implemented. A reference of a 20x20x1 k-point grid for sufficient convergence was chosen, whereby energy difference to the reference of the measured bulk platinum as a function of the k-point grid was plotted. Based on the chosen convergence of 20 meV, data from Figure 16 indicates that a number of 52 irreducible k-points, representing a 10x10x1 k-point grid serves as optimal for the studied system.

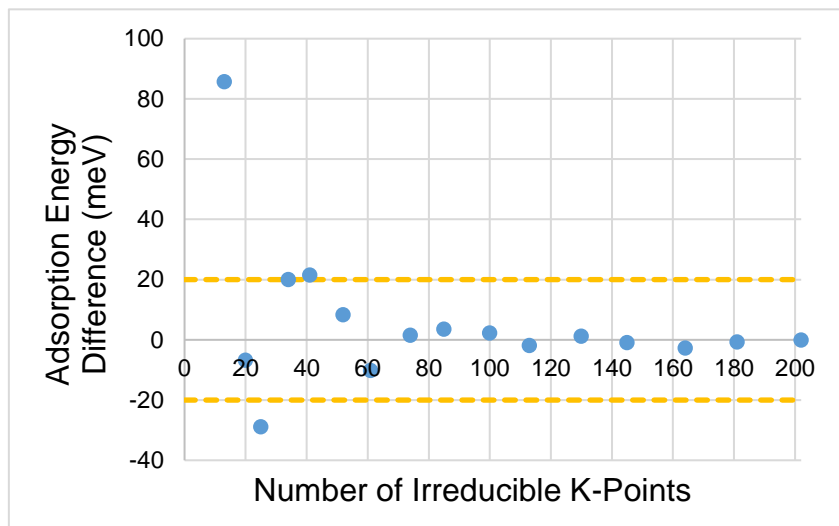


Figure 16: Adsorption Energy Difference Versus Number of Irreducible K-Points (BLUE) for Pt(111) measured from diatomic oxygen adsorption at 0.25ML on a 2x2 Pt surface with a vacuum spacing of 14 Å, cut-off energy of 400 eV, with 6 layers, 2 relaxed. Reference at a 20x20x1 k-point grid.

### 3.7.2 Pt(111) Cut-Off Energy

Cut-off energy optimisation for Pt(111) was achieved in a similar manner to that of Pt(100), using a conventional unit cell for bulk platinum with a lattice parameter of 3.981 Å. The investigated unit cell was set with an identical k-point grid of 10x10x1 to ensure that a sufficient number of irreducible k-points were available, as well as a vacuum spacing of 14 Å to ensure sufficient basis for convergence. The investigated system was a 5-layered platinum slab with 2 relaxed layers, where adsorption of diatomic oxygen at 0.25 ML was implemented. Measurements of the total energy of the system at varying cut-off energies was implemented. The same reference cut-off energy of 500 eV for sufficient convergence was chosen, whereby energy difference to the reference of the measured bulk platinum as a function of cut-off energy was plotted. Based on the chosen convergence of 20 meV, data from Figure 17 indicates that a cut-off energy of 400 eV serves as optimal for the studied system.

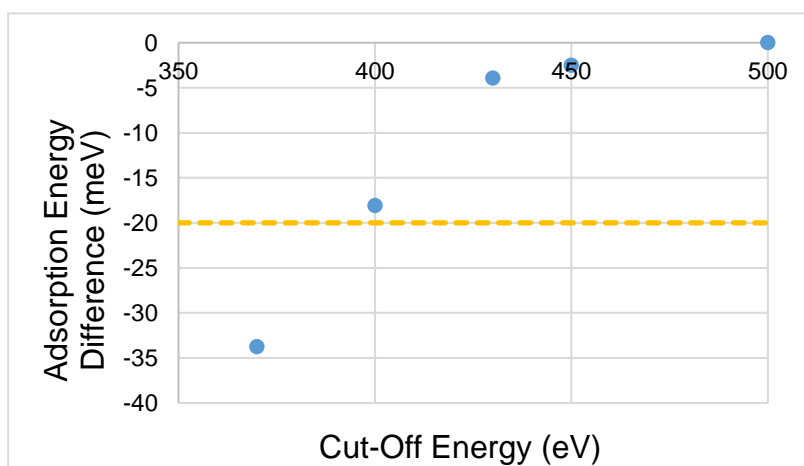


Figure 17: Adsorption Energy Difference Versus Cut-Off Difference (BLUE) for Pt(111) measured from diatomic oxygen adsorption at 0.25ML on a 2x2 Pt surface with a vacuum spacing of 14 Å, k-point grid of 1010x1, with 6 layers, 2 relaxed. Reference at a 500eV slab.

### 3.7.3 Pt(111) Number of Layers

An optimal number of layers was considered for the Pt(111) surface based on the same reasoning for that of Pt(100). As with the Pt(100) surface, 12 layers was chosen to overestimate the accuracy of the system and was thus chosen as a convergence reference. The adsorption energy was calculated for Pt(100) at 0.25 ML for all number of layers between 3 and 12; using a cut-off energy of 400 eV, a k-point grid of 10x10x1, a vacuum spacing of 14 Å and 2 relaxed layers. The same convergence of 20 meV for the adsorption energy difference to that of the 12 layered system was implemented for the Pt(111) surface to that of the Pt(100) surface. The adsorption energy was calculated for Pt(111) for all number of layers between 3 and 12 similar to that of Pt(100). The adsorption energy difference versus number of layers for a Pt(111) surface is plotted in Figure 18, where the adsorption energy difference of -250 meV for 3 layers is omitted. Based on this data, the number of layers converges to the desired energy difference of 20meV when 6 layers are used to create the Pt slab. As computational time increases steadily upon increasing the number of layers, 6 layers serves as an optimum value which minimises computational time while achieving the desired accuracy

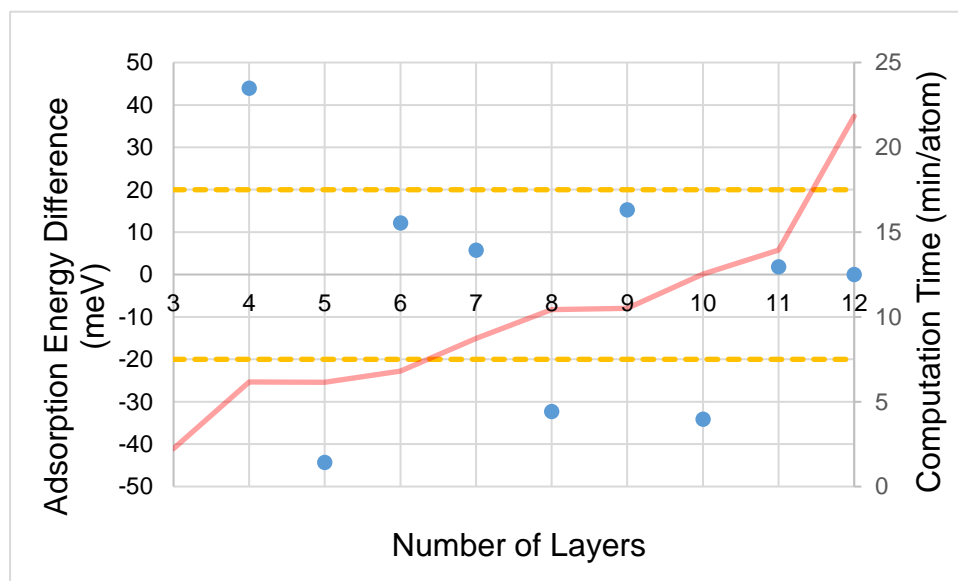


Figure 18: Adsorption energy difference versus number of layers (BLUE) for Pt(111), measured from diatomic oxygen adsorption at 0.25ML on a 2x2 Pt surface with a vacuum spacing of 14 Å with 2 relaxed layers. K-point grid of 10x10x1 and cut-off energy of 400 eV. Reference at a 12-layered slab. Computational Time against number of layers additionally plotted (RED)

### 3.7.4 Pt(111) Number of Relaxed Layers

An optimal number of relaxed layers was considered for the Pt(111) surface based on the same reasoning for the Pt(100) surface. As with the Pt(100) surface, a number of 5 relaxed layers was chosen as an overestimation to accurately model the system and was thus used as a reference point. Adsorption energy was investigated through adsorption of diatomic oxygen on Pt(100) at 0.25 ML. This system implemented a cut-

off energy of 400 eV, a k-point grid of 10x10x1 and a vacuum spacing of 14 Å. An optimal number of relaxed layers would present adsorption energies within 20 meV to that of 5 relaxed layers, indicating sufficient convergence. Adsorption energy difference against a system with 5 relaxed layers is plotted against the number of relaxed layers for Pt(111) in Figure 19, where based upon the chosen convergence of 20 meV, 2 relaxed layers has been chosen as optimal for the surface, minimising computational time while achieving desired accuracy

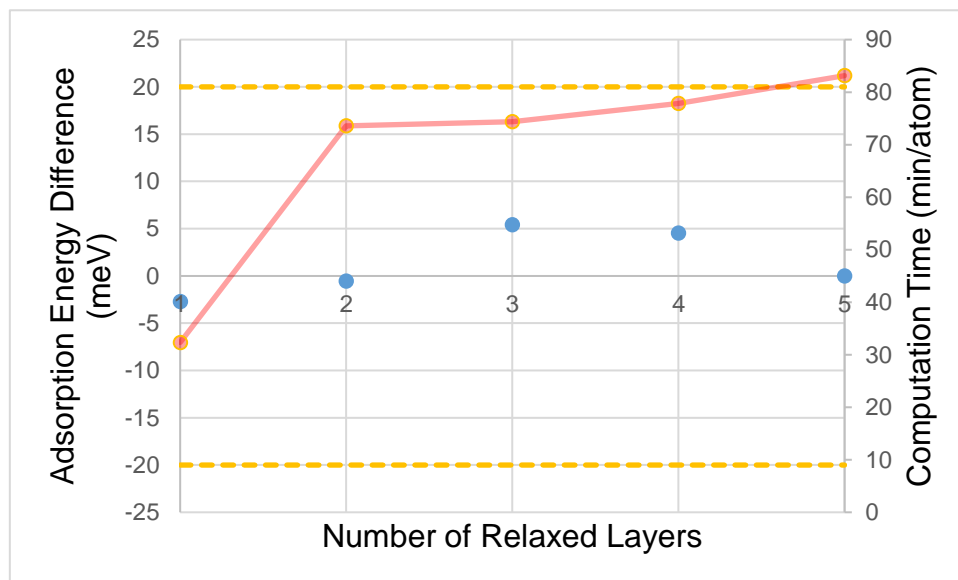


Figure 19: Adsorption energy difference against the number of relaxed layers (BLUE) in Pt(111), measured from diatomic oxygen adsorption at 0.25 ML on a 2x2 Pt surface with a 14 Å vacuum spacing with 6 layers and a cut-off energy of 400 eV. Reference at a 5-relaxed layered slab. Computational Time against number of layers additionally plotted (RED)

### 3.7.5 Pt(111) Vacuum Spacing

Optimisation of vacuum spacing for the Pt(111) surface was considered based on similar reasoning to that of the Pt(100) surface. Vacuum spacing of 14Å was chosen as the reference for this study identical to that of Pt(100). Adsorption of diatomic oxygen on a Pt(100) surface was 5 layers, 2 relaxed, at 0.25 ML was investigated with a k-point grid of 10x10x1 and cut-off energy of 400 eV. Adsorption energy difference against a 14Å vacuum spaced unit was plotted against various vacuum spacings ranging from 10-14Å for Pt(111) and is presented in Figure 20. It must be noted that a considerably high adsorption difference of -33.5 meV for 10 Å vacuum spacing on Pt(111) was recorded, and as such this recording has been excluded from the plot. Based on the convergence of 20 meV, adsorption energy differences are within the desired convergence at 11Å. In order to ensure consisting optimised parameter choices for both surfaces, a vacuum spacing of 11Å was chosen to optimise the Pt(111) and the Pt(100) surfaces. This choice is validated by the small computational time difference between 10 and 11 Å vacuum spacing for both Pt(100) and Pt(111) surfaces, whereby using 11 Å vacuum spacing for both surfaces allows for simple comparison between the surfaces at a desired accuracy with negligible addition to computational time.

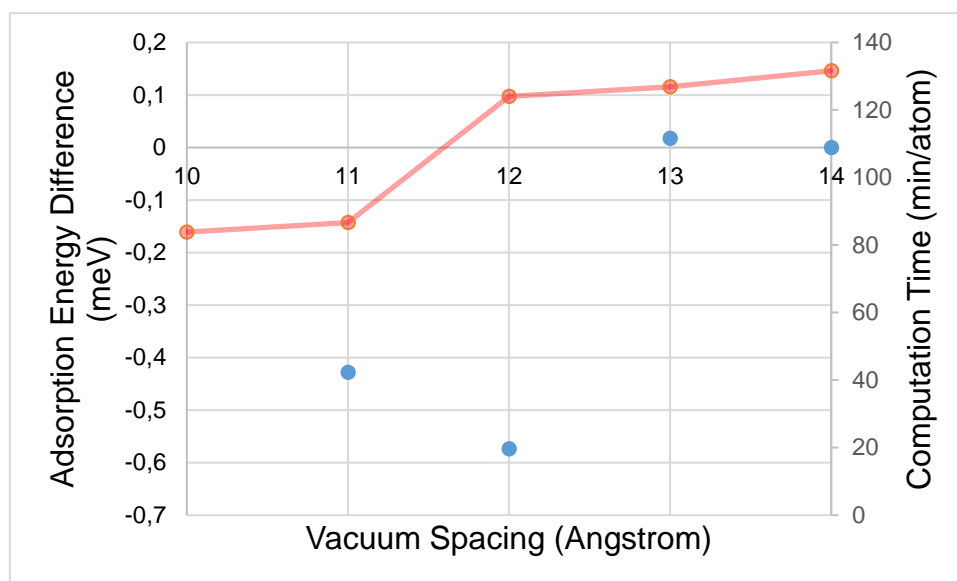


Figure 20: Adsorption Energy Difference versus Vacuum Spacing (BLUE) for Pt(111), measured from diatomic oxygen adsorption at 0.25ML on a 2x2 Pt surface with a cut-off energy of 400 eV and a k-point grid of 10x10x1, with 5 layers, 2 relaxed. Reference at a 14 Å slab. Computational Time against number of layers additionally plotted (RED)

### 3.8 Summary of Optimised Model for Pt(100) and Pt(111)

From the optimisation methodology, optimised models for both Pt(100) and Pt(111) were determined. The optimised parameters for the determined models are summarised in Table 2, and will be used within the study for obtaining of results.

Parameter	Pt(100)	Pt(111)
K-points	10x10x1	10x10x1
Cut-off Energy (eV)	400	400
Number of Layers	6	6
Number of Relaxed Layers	2	2
Vacuum Spacing (Å)	11	11

Table 2: Summary of the optimised parameters for the optimised models of Pt(100) and Pt(111)

### 3.9 Determination of Preferred Adsorption Sites and Adsorption Energies

Given that an optimised model has been established, the DFT study can now be used to accurately understand the preferred adsorption sites and their associated energies. The system will be modelled using a 2x2 unit cell, which therefore contains four platinum atoms per layer. This study aims to understand how the adsorption of diatomic oxygen on platinum changes at varying coverages. Consequently, a coverage of 0.25 ML, where one diatomic oxygen molecule is bonded to a platinum surface with four Pt atoms, will first be investigated. All four possible adsorption sites for the Pt(111) surface and all three possible adsorption sites for the Pt(100) surface will be tested at a coverage of 0.25 ML. An example of one of these seven systems that must be tested

is shown below in Figure 21 which represents diatomic oxygen adsorbed on Pt(111) on an hcp site. Please note that in all cases only one oxygen atom is bonded to the site of interest, while the other is diatomically bonded to adsorbed oxygen atom.

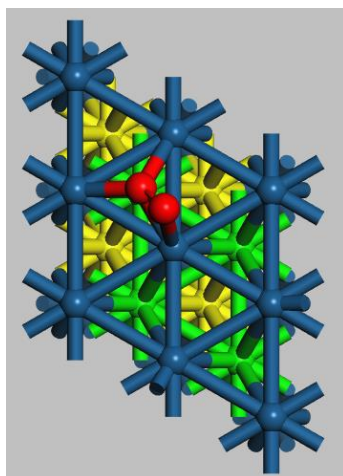


Figure 21: A Pt(111) surface with diatomic oxygen adsorbed on a hcp site at a coverage of 0.25 ML

Once all seven systems at a coverage of 0.25 ML have been tested, each system must then be checked for stability. The *VASP* returns the final geometry of each simulation; consequently, if the adsorbed oxygen remained on the initial site, then it is considered stable in that site and an adsorption energy can be calculated for this site. Subsequently, the adsorption energies for every stable site can be calculated and the one with the lowest energy value, and most thermodynamically stable, represents the preferred adsorption site for diatomic oxygen on each Pt surface at a coverage of 0.25 ML.

It is then assumed that the most preferred adsorption site at 0.25 ML is also the most thermodynamically site at higher coverages. This assumption is based on the concept that at higher coverages all adsorption sites will become less stable and relative to each other the lowest energy site will remain the lowest. Subsequently, all possible configurations of this adsorption site must then be tested at coverages of 0.50 ML, 0.75 ML and 1.00 ML. The most stable configuration at each coverage, based on the lowest adsorption energy, can then be assumed to be the preferred geometry at this coverage. Consequently, the most preferred adsorption sites and their associated energies at varying coverages have now been obtained and can be used to determine the operating conditions at which certain configurations are most thermodynamically stable.

### 3.10 Thermodynamic Correlations

It must be noted that *VASP* operates at a temperature of 0K. Consequently, all the adsorption energies and preferred adsorption sites determined up to this point are only true at 0 K. Therefore, thermodynamic correlations presented by Hirano (1993) and by

Sandler (2006) will be used to produce the Gibbs energy of adsorption at varying temperatures and pressures. This will allow the stability of the sites to be tested at varying conditions, and consequently the conditions at which full coverage is possible can be found. The lowest Gibbs energy indicates the most thermodynamically preferred system, which is vital to this study; furthermore, a positive Gibbs energy indicates that the oxygen would prefer to remain in the gas phase than adsorb on the surface. Therefore, the calculation of the Gibbs energy of the system will aid the development of this study's objectives by providing operations conditions at which various coverages are possible.

In order to calculate the Gibbs energy of adsorption, the following equation must be used:

$$G(T, P)_{\text{adsorption}} = G(T, P)_{\text{adsorbed slab}} - G(T, P)_{\text{clean slab}} - G(T, P)_{\text{diatomic oxygen}} \quad (10)$$

All three individual Gibbs energies required can be calculated via the following equation:

$$G(T) = H(T) - T.S \quad (11)$$

*VASP* provides the enthalpy of a system at 0K ( $E_{\text{elec}}$ ), consequently, this enthalpy needs to be corrected and upscaled to various temperatures as follows:

$$H(T) = E_{\text{electronic}} + E_{\text{vibrational}}(T) + E_{\text{rotation}}(T) + E_{\text{translation}}(T) + RT \quad (12)$$

$$E_{\text{vibration}}(T) = \frac{1}{2} N_A \sum_i h\nu_i + N_A \sum_i \frac{h\nu_i \cdot \exp(-\frac{h\nu_i}{k_B T})}{1 - \exp(-\frac{h\nu_i}{k_B T})} \quad (13)$$

$$E_{\text{rotation}}(T) = \frac{n_{\text{rot}}}{2} RT \quad (14)$$

$$E_{\text{translation}}(T) = \frac{3}{2} RT \quad (15)$$

A vibrational analysis will be carried out on each system on *VASP* in order to determine the different frequencies ( $\nu_i$ ) required for the calculations shown above.

Once the enthalpy is obtained at a specific temperature, the entropy can be found as follows:

$$S(T) = S_{\text{vibration}}(T) + S_{\text{rotation}}(T) + S_{\text{translation}}(T) + S_{\text{degeneracy}} \quad (16)$$

$$S_{\text{vibration}} = R \sum_i \frac{\frac{h\nu_i}{k_B T} \exp(-\frac{h\nu_i}{k_B T})}{1 - \exp(-\frac{h\nu_i}{k_B T})} - R \sum_i \ln \left( 1 - \exp\left(-\frac{h\nu_i}{k_B T}\right) \right) \quad (17)$$

$$S_{\text{rotation}}(T) = R \cdot \ln \left( \frac{8\pi^2 I_x k_B T}{\sigma h^2} \right) + R \quad (18)$$

$$S_{\text{translation}}(T) = R \left( \ln \left( \left( \frac{2\pi k_B T M_w}{h^2 N_A} \right)^{\frac{3}{2}} \cdot \frac{k_B T}{P} \right) + \frac{5}{2} \right) \quad (19)$$

$$S_{\text{degeneracy}}(T) = R \cdot \ln(g) \quad (20)$$

Once both the enthalpy and entropy is calculated at a specific temperature, using the electronic energy and vibrational analysis provided by *VASP*, the Gibbs energy of each system can be determined. Subsequently, this process can be repeated for an adsorbed slab, a clean slab and diatomic oxygen in the gas phase, in order to determine the Gibbs energy of adsorption as outlined in Equation 10. However, it must be noted that only pure diatomic oxygen in the gas phase will take into consideration effects due to rotation and translation. It is assumed that molecules in the gas phase are free to vibrate and move in all directions, giving rise to vibrations, rotations and translations. However, when an atom molecule is adsorbed on a Pt surface, it is restricted by its bond to the surface and is assumed to vibrate only. Consequently, the calculation of the Gibbs energy of the adsorbed slab will only include vibrational effects. Furthermore, it is assumed that the Pt atoms, both on the surface and below the surface, are fixed and cannot move freely due to their interactions with a much larger bulk Pt structure.

Once the Gibbs energy of adsorption has been determined as a function of temperature and pressure using the thermodynamic models described above, then a surface phase diagram can be generated which aids the understanding the most stable configurations at specific operating conditions.

## 4. Results and Discussion for Pt(100)

### 4.1 Adsorption Energies and Preferred Adsorption Sites for Pt(100)

#### 4.1.1 Pt(100) at 0.25 ML Coverage

The optimised model for the Pt(100) surface was first used to test the preferred adsorption site at a coverage of 0.25 ML. Given that a 2x2 unit cell was used in this study, there were four Pt atoms on the surface of all simulated systems; consequently, a coverage of 0.25 ML was obtained when one diatomic oxygen was adsorbed on the surface. It was decided that the starting geometry submitted to *VASP* will only include one oxygen atom bonded to the site of interest, with the other atom diatomically bonded to this adsorbed oxygen atom. Figure 22 below shows the top and side views of the initial starting geometries for all three sites tested at a coverage of 0.25 ML on Pt(100). For all initial geometries tested, the bond length between the adsorbed oxygen and the Pt surface was kept at a constant 2.10 Å while the bond length between the two diatomically bonded oxygen atoms was kept at constant 1.23 Å, in order to provide consistency in the simulations.

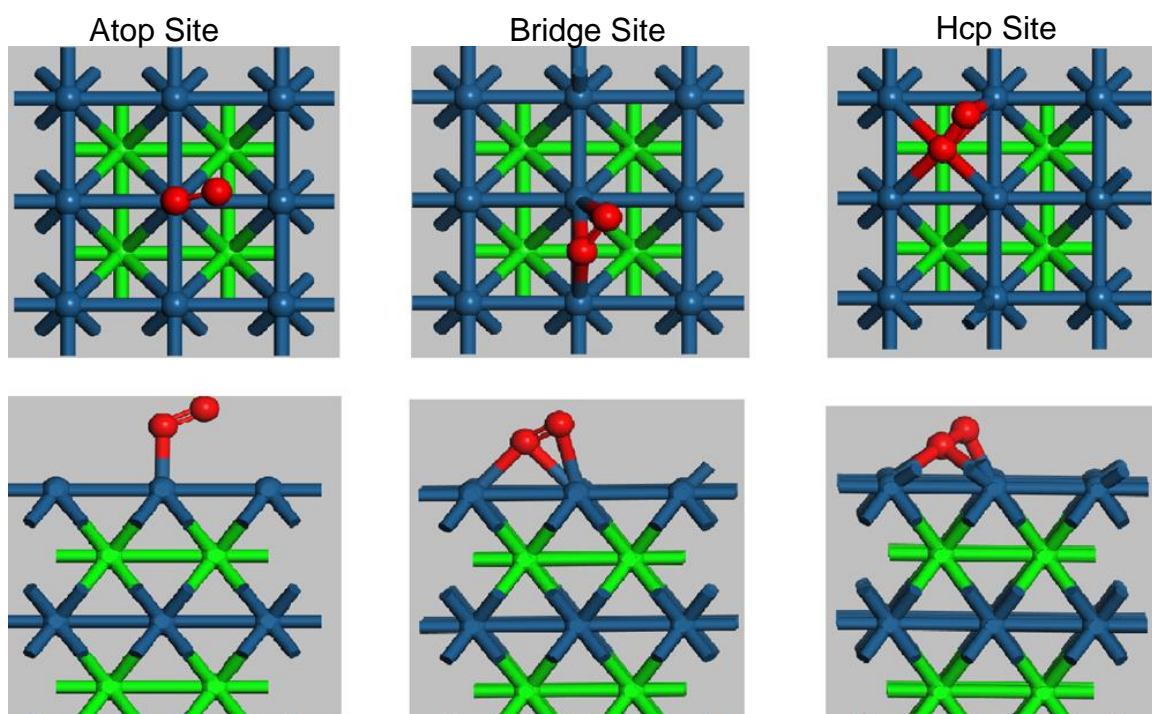


Figure 22: Top (above) and side (below) views of the initial geometries of all three possible adsorption sites tested at a coverage of 0.25 ML on the Pt(100) surface

All three of these starting geometries had their energies calculated in an effort to test the preferred adsorption site for the Pt(100) surface. It must be noted that for the atop adsorption site, the second oxygen not bonded to the surface was pointed towards a bridge; for the bridge site the second oxygen was pointed towards an hcp site and also bonded to the atop site; while for the hcp site, the second oxygen was bonded to and pointing towards another atop site. It was a concern that changing the configuration of this second oxygen atom may alter the final geometry solved for the system. However,

all possible configurations for the position of this second oxygen atom were tested and it was found that the system reached the same final geometry. Consequently, only the energy and final geometry of the three configurations shown above in Figure 22 will be reported.

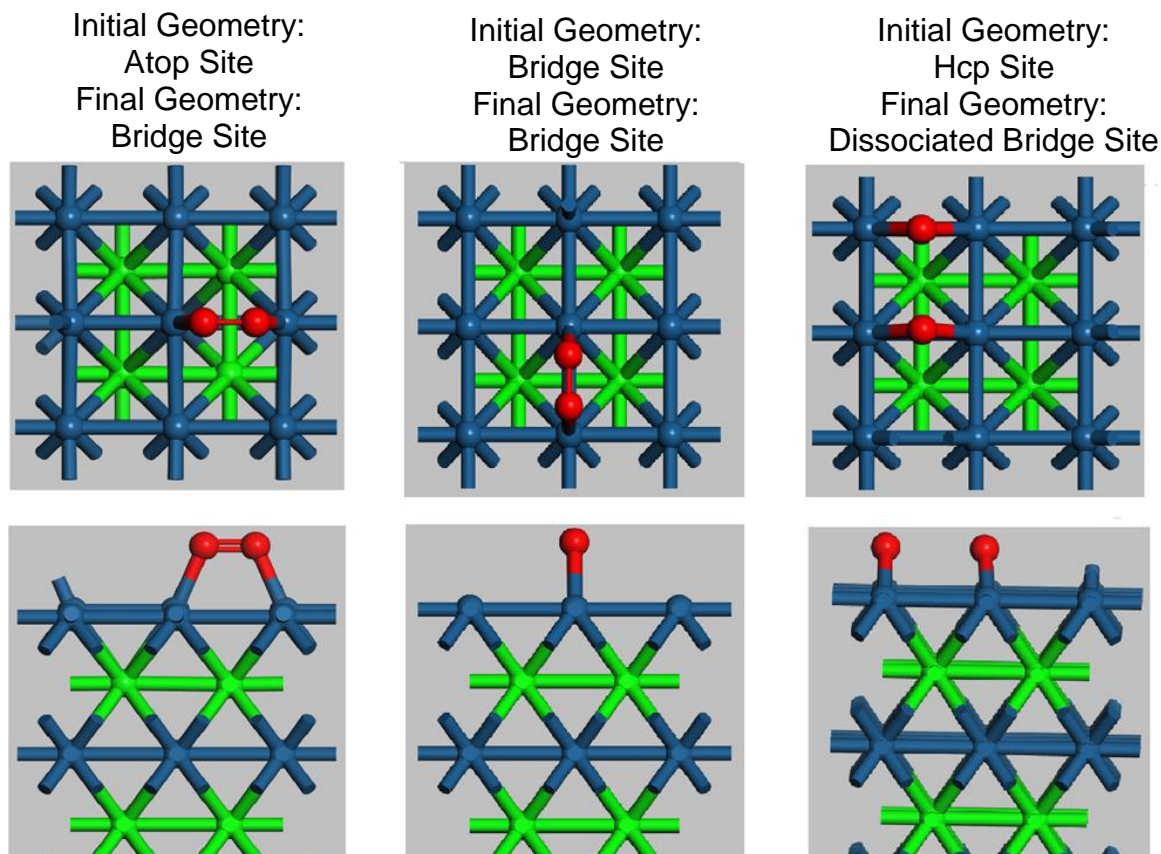


Figure 23: Top (above) and side (below) views of the final geometries of all three possible adsorption sites tested at a coverage of 0.25 ML on the Pt(100) surface

Figure 23 above shows the final geometries for all three systems that were tested, as shown in Figure 22, in order to determine the most stable adsorption site at 0.25 ML. *VASP* continuously iterated the geometry of the initial system, calculating the total system energy at each iteration, until an energy minimum was found and the system could be considered stable. Consequently, as is clear from Figure 23, both the hcp and the atop adsorption sites on the Pt(100) surface cannot be considered stable. When the oxygen was initially adsorbed on an atop site, it moved to a single bridge site with both oxygen atoms sitting above the same bridge and still diatomically bonded, as can be from Figure 23. The system which initially had an oxygen atom over a hcp site, as seen in Figure 22, also ended on a bridge site; however, the oxygen atoms dissociated and went to two separate bridge sites, as shown in Figure 23. While the system which started with one oxygen atom over a bridge site, had a final geometry consisting of both oxygen atoms adsorbed over a single bridge site, as seen in Figure 23. These results indicate that adsorption of diatomic oxygen on the Pt(100) surface is only thermodynamically stable over a bridge site. However, the energies of these results

need to be explored to understand which configuration of bridge site adsorption is more stable.

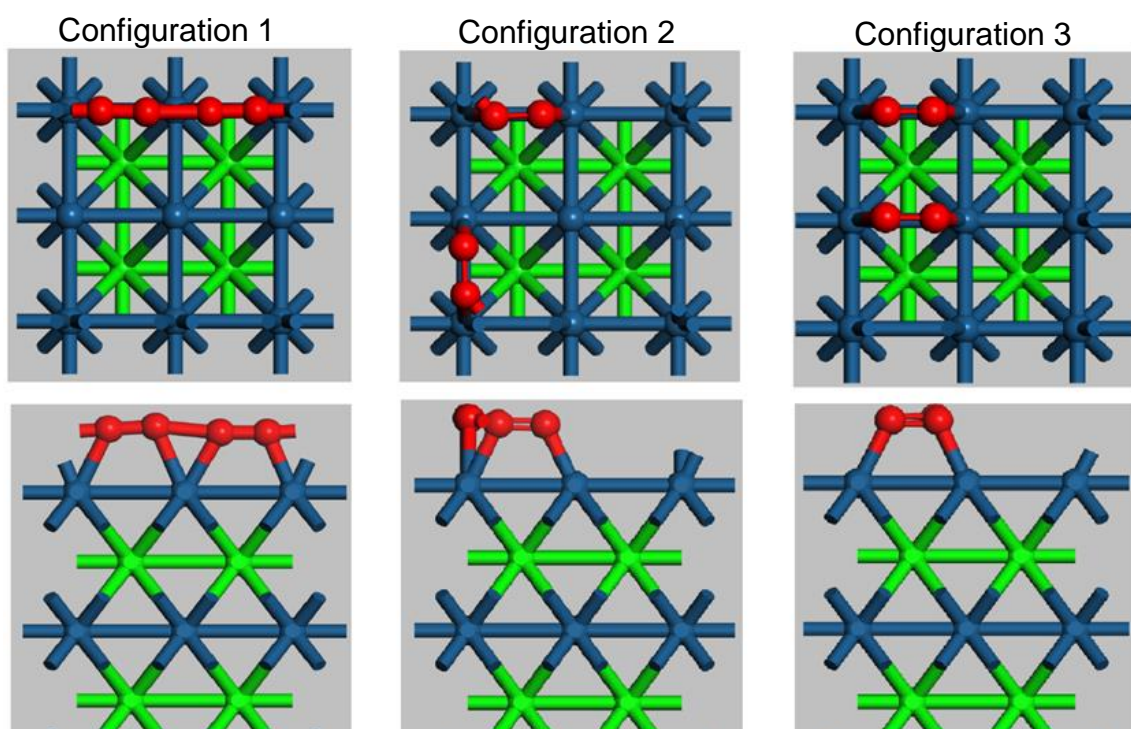
Table 3: Description of the geometries of all systems tested at a coverage of 0.25 ML on the Pt(100) surface and their associated adsorption energies at 0 K

<b>Description of Initial Geometry</b>	<b>Description of Final Geometry</b>	<b><math>G_{adsorption}</math> at 0 K</b>
One oxygen atom adsorbed to an atop site diatomically bonded to another oxygen atom facing a bridge site	Two oxygen atoms adsorbed on the Pt surface over a single bridge site and diatomically bonded to each other	-1.14 eV
One oxygen atom adsorbed over a bridge site diatomically bonded to another oxygen atom facing a hcp site	Two oxygen atoms adsorbed on the Pt surface over a bridge single site and diatomically bonded to each other	-1.14 eV
One oxygen atom adsorbed to the Pt surface over a hcp site diatomically bonded to another oxygen atom facing an atop site	Dissociative adsorption of diatomic oxygen with both oxygen atoms adsorbed over two separate bridge sites on the Pt surface	-0.93 eV

Table 3 describes the final geometry of all three systems tested and gives its associated Gibbs energy of adsorption 0 K in order to highlight the most stable adsorption site at 0.25 ML. The dissociative adsorption of oxygen over two bridge sites (initially bonded to a hcp site) had a slightly higher energy than that of the bridge site adsorption where the oxygen atoms remained diatomically bonded. Consequently, this configuration, as shown in Figure 23, has been proven to be the preferred adsorption site for diatomic oxygen on the Pt(100) surface as it has the lowest adsorption energy and is therefore the most thermodynamically stable. Therefore, from this point forward, it will be assumed that this adsorption site is the most stable for all coverages tested. Furthermore, when referring to the Pt(100) surface, a bridge site will be defined as the configuration labelled in Figure 23 as a bridge site, which consists of two diatomically bonded oxygen atoms over a single bridge site. Additionally, the final geometry of this bridge site configuration showed a Pt-O bond length of 1.99 Å and a O-O diatomic bond length of 1.36 Å. These bond lengths were used to formulate the initial geometries at higher coverages.

### 4.1.2 Pt(100) at 0.50 ML Coverage

It was then assumed that this bridge site will continue to be the most stable adsorption site at all higher coverages. This is a fair assumption considering that all other sites tested at a coverage of 0.25 ML were unstable and tended towards this bridge site. Consequently, this bridge site was tested at a coverage of 0.50 ML. In order to gauge the most stable system at this coverage, all possible configurations of this bridge site were simulated and the configuration with the lowest Gibbs adsorption energy was then considered to be the most stable at this coverage. Given the bridge site defined above, there were eight possible configurations at a coverage of 0.50 ML which were all tested. The top and side views of the initial geometries all eight bridge site configurations tested are shown in Figure 24 below. Each configuration is simulated by using the same Pt-O and O-O bond lengths that were found in the final geometry of the bridge site in Figure 23. These bond lengths are set in order to ensure consistency when comparing the different configurations as well as to minimise computational time required as these bond lengths should lead to an initial geometry which is as close to the final geometry as possible.



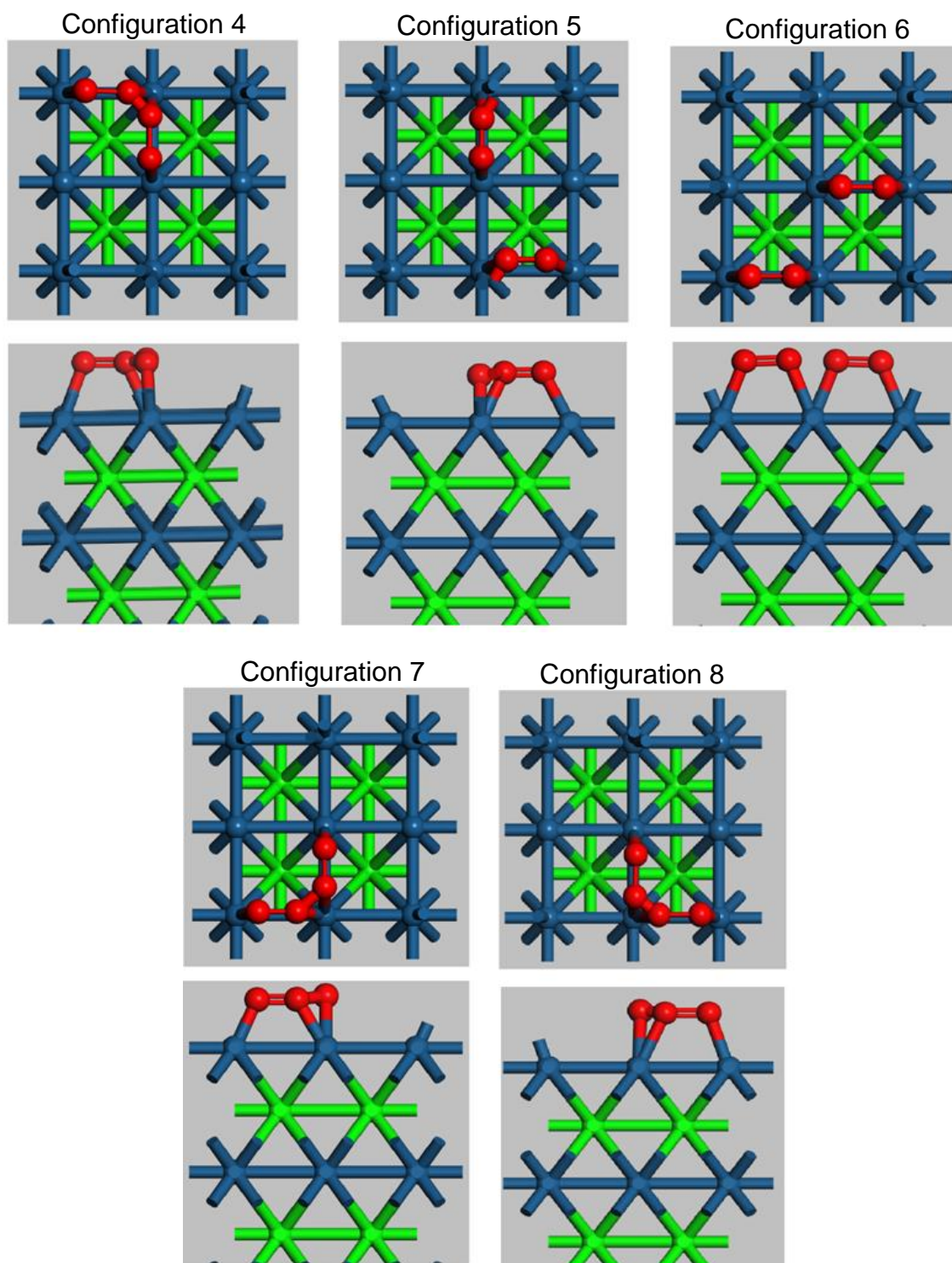


Figure 24: Top (above) and side (below) views of the initial geometries of all eight bridge site configurations tested at a coverage of 0.50 ML on the Pt(100) surface

All eight of the initial geometries given in Figure 24 were run using *VASP* in order to understand the most stable configuration on the Pt(100) surface at a coverage of 0.50 ML. The thermodynamic stability of each configuration was investigated by comparing their adsorption energies at 0 K, as shown in Table 4 below.

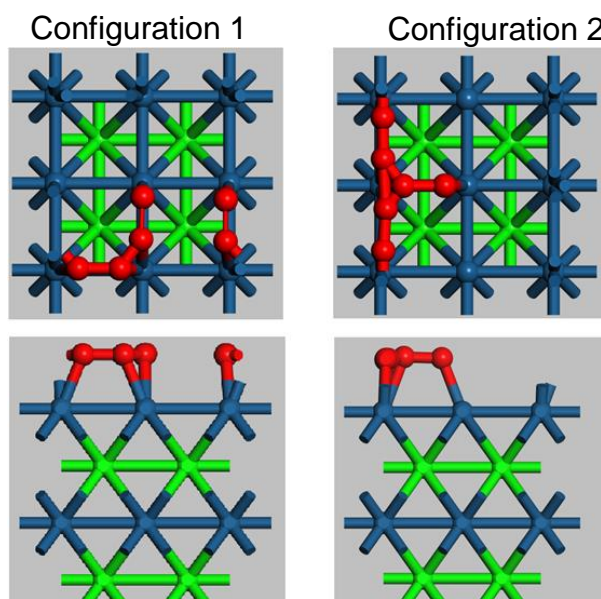
Table 4: Adsorption energies at 0 K for all eight configurations tested at a coverage of 0.50 ML on the Pt(100) surface

Configuration Number	$G_{adsorption}(0K)$
1	Unstable
2	-1.30 eV
3	-2.24 eV
4	-1.30 eV
5	-1.05 eV
6	-1.92 eV
7	-1.05 eV
8	-2.11 eV

As can be seen from Table 4, all configurations tested except for configuration 1 were stable. Configuration 1 resulted in a final geometry where one of the oxygen species was not bonded to the surface, making it inapplicable to understanding the nature of adsorption on Pt(100) at 0.50 ML, and is therefore labelled as unstable. However, all other configurations resulted in a final geometry at 0.50 ML and their adsorption energies were reported. As is evident from Table 3, configuration 3 resulted in the lowest energy of adsorption and is therefore the most thermodynamically stable geometry at this coverage. It must also be noted that the final position of configuration 3 is the same as the initial geometry that can be seen in Figure 24, with the Pt-O and O-O bond lengths also remaining unchanged.

#### 4.1.3 Pt(100) at 0.75ML Coverage

The bridge site, as defined in Section 4.1.1, was then once again assumed to be the preferred adsorption site at a coverage of 0.75 ML. Consequently, there were four unique configurations that needed to be tested in order to determine the most stable geometry at this coverage. The top and side views of the initial geometries of all four unique configurations that were considered are shown in Figure 25 below.



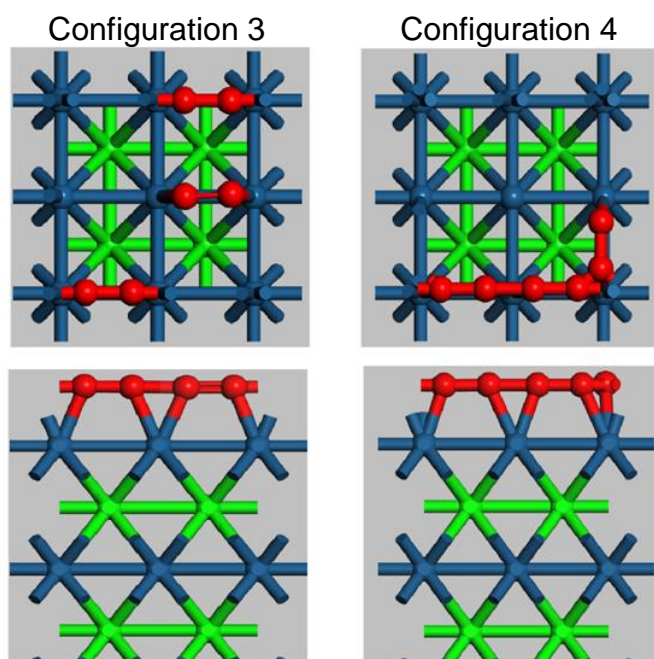


Figure 25: Top (above) and side (below) views of the initial geometries of all four bridge site configurations tested at a coverage of 0.75 ML on the Pt(100) surface

Due to strong electrostatic interactions between oxygen atoms, it was expected that these configurations may be unstable and a coverage of 0.75 ML may not be possible. Table 5 outlines the adsorption energy at 0 K for each stable configuration; and it can be seen that both configuration 2 and 3 were unstable. For both configurations 2 and 3, the final geometry of the system showed that one diatomic oxygen desorbed off the surface, making this geometry unstable when considering a coverage of 0.75 ML. However, both configuration 1 and 4 were stable and resulted in final geometries in which all six oxygen atoms were still adsorbed to the surface; consequently, adsorption energies are reported for these geometries.

Table 5: Adsorption energies at 0 K for all four configurations tested at a coverage of 0.75 ML on the Pt(100) surface

Configuration Number	$G_{adsorption}(0K)$
1	-1.89 eV
2	Unstable
3	Unstable
4	-2.13 eV

As is clear from Table 5, configuration 4 resulted in the lowest adsorption energy, and was therefore considered the most stable configuration at a coverage of 0.75 ML. Figure 26 below shows the final geometry of the configuration 4, and it can be seen that one of the diatomic oxygen molecules dissociated and adsorbed to two separate bridge sites, while the other two diatomic oxygens adsorbed over atop sites, which is very different to the initial geometry which can be seen in Figure 25. This configuration is the most stable adsorption geometry at a coverage of 0.75 ML, and has an associated adsorption energy of -2.13 eV at 0 K.

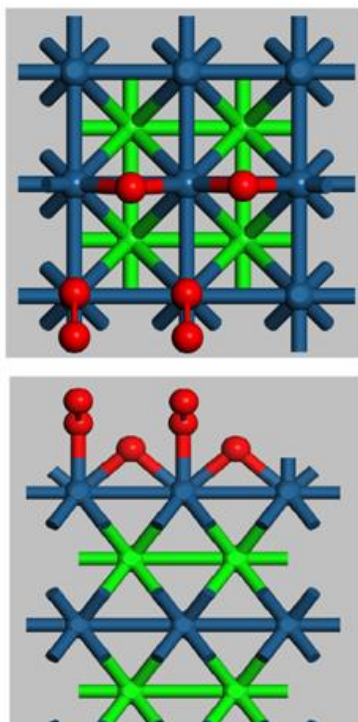


Figure 26: Top (above) and side (below) view of the final geometry of configuration 4 (most stable) of the configurations tested at a coverage of 0.75 ML on the Pt(100)

#### 4.1.4 Pt(100) at 1.00ML Coverage

The bridge site, as defined in Section 4.1.3, is once again used as a starting point to test possible geometries at a coverage of 1.00 ML, given that it was proven to be the most stable adsorption site at lower coverages. Three unique configurations were tested at full coverage using the pre-defined bridge site, and the side and top views of the initial geometries of all three configurations tested are shown in Figure 27 below.

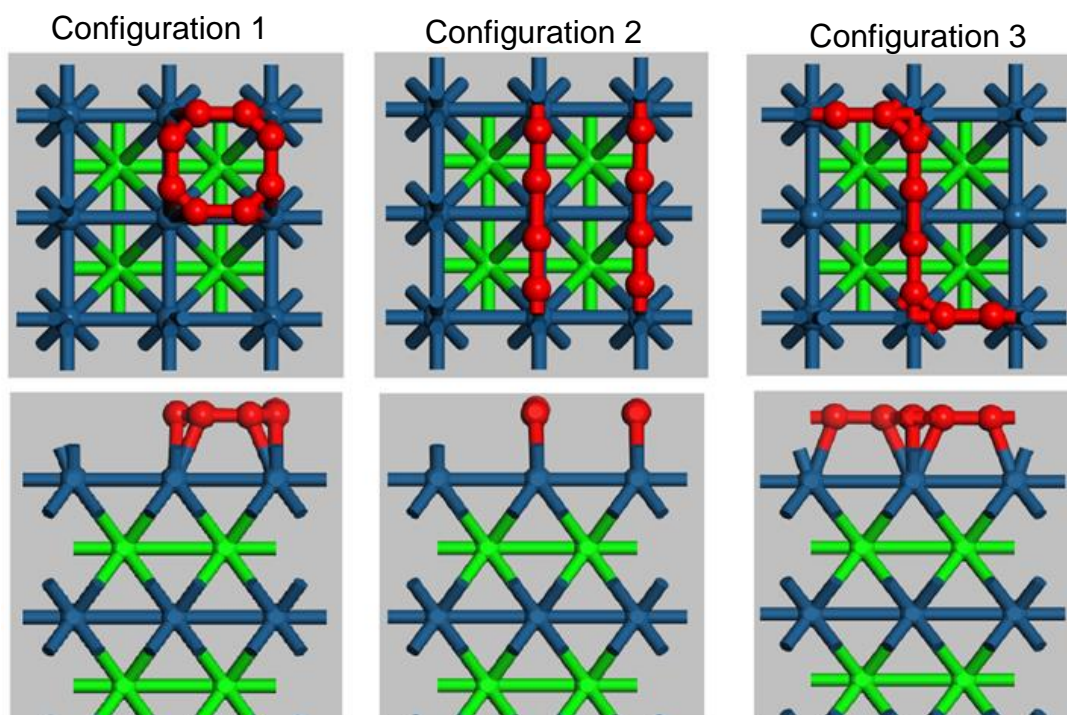


Figure 27: Top (above) and side (below) views of the initial geometries of all three bridge site configurations tested at a coverage of 1.00 ML on the Pt(100) surface

All three of the configurations at full coverage, shown in Figure 27, were run on *VASP*. Due to strong electronic interactions between oxygen atoms, none of the three geometries remained stable and full coverage was not possible on the Pt(100) surface for adsorption of diatomic adsorption. Consequently, no energies are reported for these systems as full coverage was not achieved.

## **4.2 Thermodynamic Analysis of Adsorption of Diatomic Oxygen on Pt(100)**

### **4.2.1 Overview of Thermodynamics of Adsorption of Diatomic Oxygen on Pt(100)**

The most stable adsorption geometries at coverages of 0.25 ML, 0.50 ML and 0.75 ML and their associated energies at 0 K have been found. This was done by finding the preferred adsorption site at a coverage of 0.25 ML and then assuming this adsorption site will continue to be preferred at higher coverages; and subsequently testing possible configurations only for this preferred adsorption site at higher coverages. It was also found that full coverage of diatomic oxygen is not possible on the Pt(100) surface. However, all of these results are only relevant at 0 K, the temperature at which *VASP* runs. It is vital to understand what geometry is the most thermodynamically stable on the Pt(100) surface over a range of operating temperatures and pressures.

Consequently, the thermodynamic correlations provided in Section 3.10 were used to calculate the Gibbs energy of adsorption over a range of temperatures and pressures. For each coverage, the final geometry of the most stable configuration at each coverage, as determined in Sections 4.1.1-4.1.3, was used. A vibrational analysis was run on each of the final geometries in order to use the thermodynamic correlations provided in Section 3.10. Only the oxygen atoms were allowed to move freely when the vibrational analysis was run; therefore, three real vibrations were returned per oxygen atom in the system, one per plane in which it was allowed to move.

It was decided to calculate the Gibbs energy of adsorption as this provides vital information about the thermodynamic stability of the system. The lowest Gibbs energy of adsorption represents the most stable system at a particular set of operating conditions. Therefore, at a certain temperature and pressure, the coverage that can be obtained can be found by comparing the Gibbs energy of adsorption at each coverage. Furthermore, if the Gibbs energy of adsorption at all coverages is positive, then oxygen will prefer to remain in the gas phase as adsorption on the Pt surface is unstable. Therefore, the operating conditions at which no adsorption will take place can also be found.

## 4.2.2 Dependence of the Adsorption Geometry on Temperature on Pt(100)

Firstly, the dependence of temperature on the most preferred adsorption geometry was investigated at a pressure of 1 atm. Figure 28 below shows the Gibbs energy of adsorption for all three possible coverages across a range of temperatures in order to illustrate which geometry is the most stable at all reasonable operating temperatures.

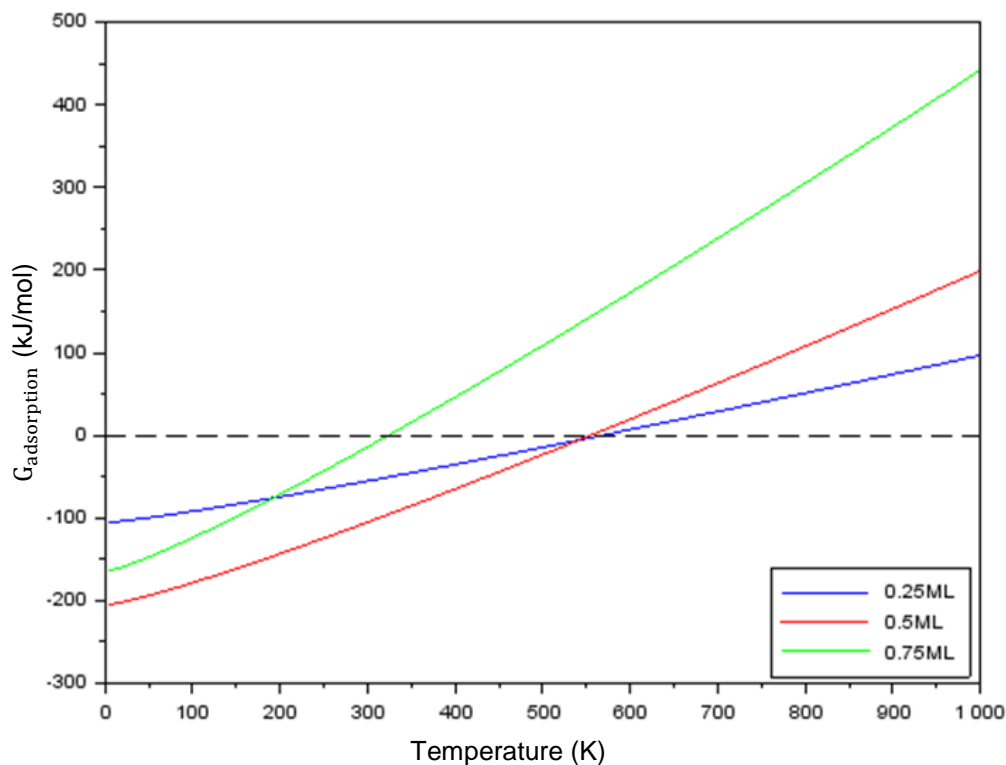


Figure 28: Gibbs energy of adsorption at 1 atm for all three possible coverages on Pt(100) over a range of temperatures

As is clear from Figure 28, there is no temperature between 0 K and 1000 K at which the Gibbs energy of adsorption for the system at 0.75 ML is the lowest. Consequently, this coverage will never be thermodynamically preferred to the other systems and it can be expected that a coverage of 0.75 ML cannot be obtained at a pressure of 1 atm. Furthermore, a coverage of 0.50 ML is the most preferred geometry for all temperatures between 0 K and 542 K at a pressure of 1 atm. This can be seen in Figure 29, which represents shows a zoomed view of Figure 28, in order to illustrate the difference between 0.50 ML and 0.25 ML more clearly. Between 542 K and 568 K, the lowest Gibbs energy adsorption is that of the 0.25 ML system; consequently, this geometry is favoured in this temperature range and at a pressure of 1 atm. As is evident from Figure 29, at any temperature higher than 568 K, the Gibbs energy of adsorption of any adsorbed system is positive; therefore, diatomic atomic will prefer to remain in the gas phase than adsorb on the Pt(100) surface.

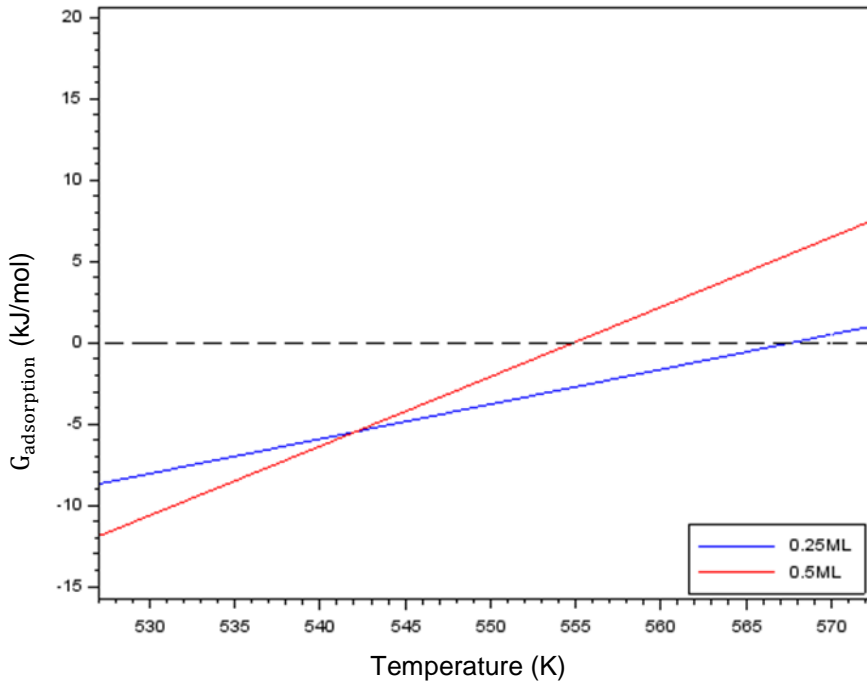


Figure 29: Zoomed in view of the Gibbs energy of adsorption at 1 atm for all three possible coverages on Pt(100) over a range of temperatures

### 4.2.3 Dependence of the Adsorption Geometry on Partial Pressure of O<sub>2</sub> on Pt(100)

Subsequently, the dependence of pressure on the preferred geometry was tested. Figure 30 shows the Gibbs energy of adsorption for all three coverages for pressures between 0 bar and 100 bar at a constant temperature of 25 °C; and it is clear that there is no pressure dependence on the most stable geometry. At all pressures under consideration, the Gibbs energy of adsorption for the 0.50 ML system is always the lowest and negative. Consequently, at a temperature of 25 °C, the Pt-O<sub>2</sub> adsorption system will always operate at a coverage of 0.50 ML regardless of the pressure.

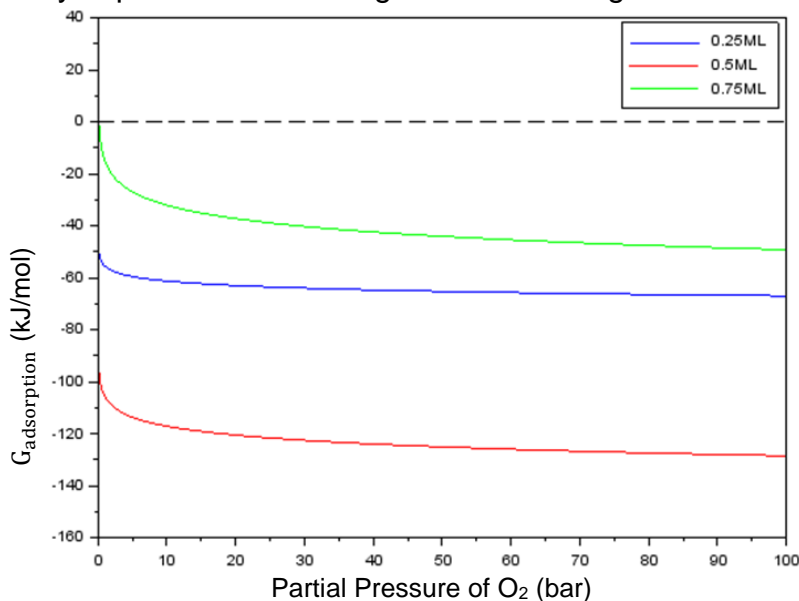


Figure 30: Gibbs energy of adsorption at 25 °C for all three possible coverages on Pt(100) over a range of pressures

### 4.3 Phase Diagram for the Adsorption of Diatomic Oxygen on Pt(100)

It is also vital to understand the simultaneous dependence of temperature and pressure on the Gibbs energy of adsorption of all three coverages tested in order to obtain a holistic overview of the operating conditions that will result in certain geometries on the Pt(100) surface. Consequently, a phase diagram was produced which relates temperature and pressure to the Gibbs energy of adsorption. A three-dimensional diagram was created which plots temperature, pressure and adsorption energy for each coverage; consequently, a surface was created for each coverage as well as a flat surface at an adsorption energy of 0 kJ/mol to serve as a reference. Figure 31 shows a side view of these surfaces, highlighting how all four surfaces interact on a three-dimensional plot.

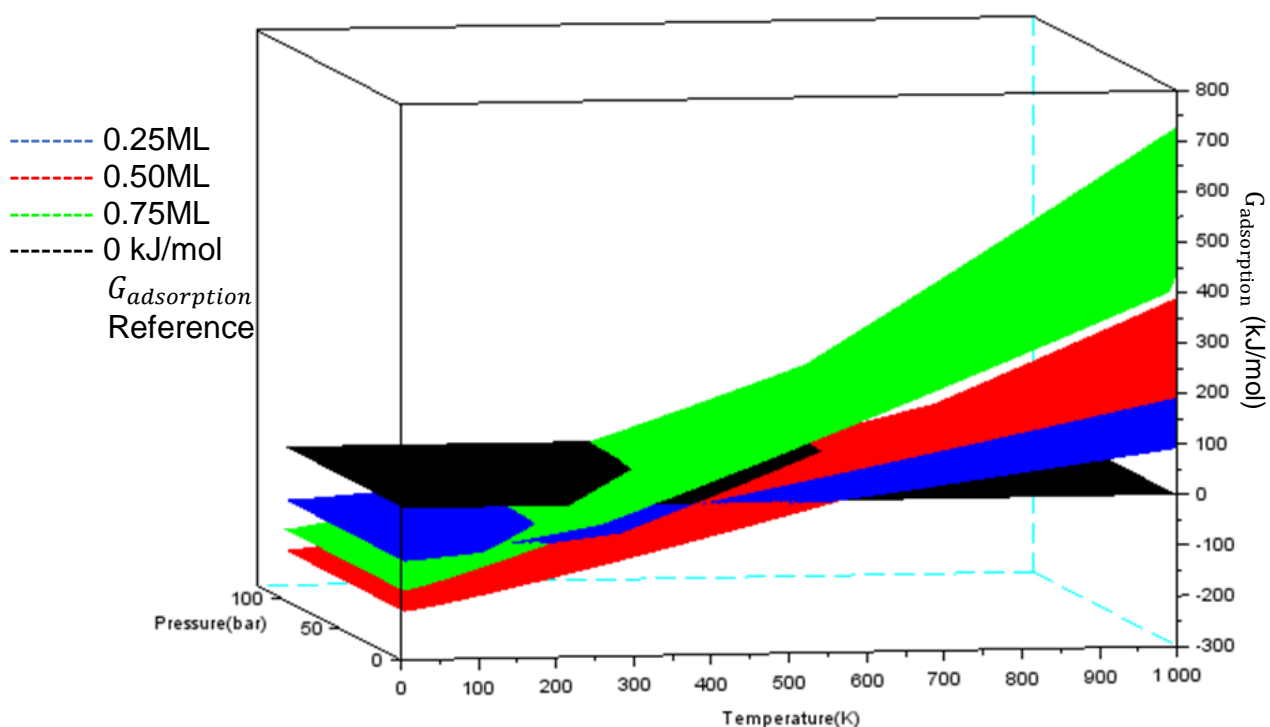


Figure 31: Side view of the three-dimensional plot of all interacting surfaces used to develop the phase diagram for Pt(100)

The most thermodynamically stable system, given a particular set of operating conditions, is always represented by the geometry with the lowest adsorption energy, given that this adsorption energy is negative. Consequently, this three-dimensional plot was used to generate a phase diagram, as shown in Figure 32, which was developed by rotating the three dimensional plot such that the lowest surface is always viewed. This allows the illustration of the most stable operating geometry at any reasonable combination of temperatures and pressures.

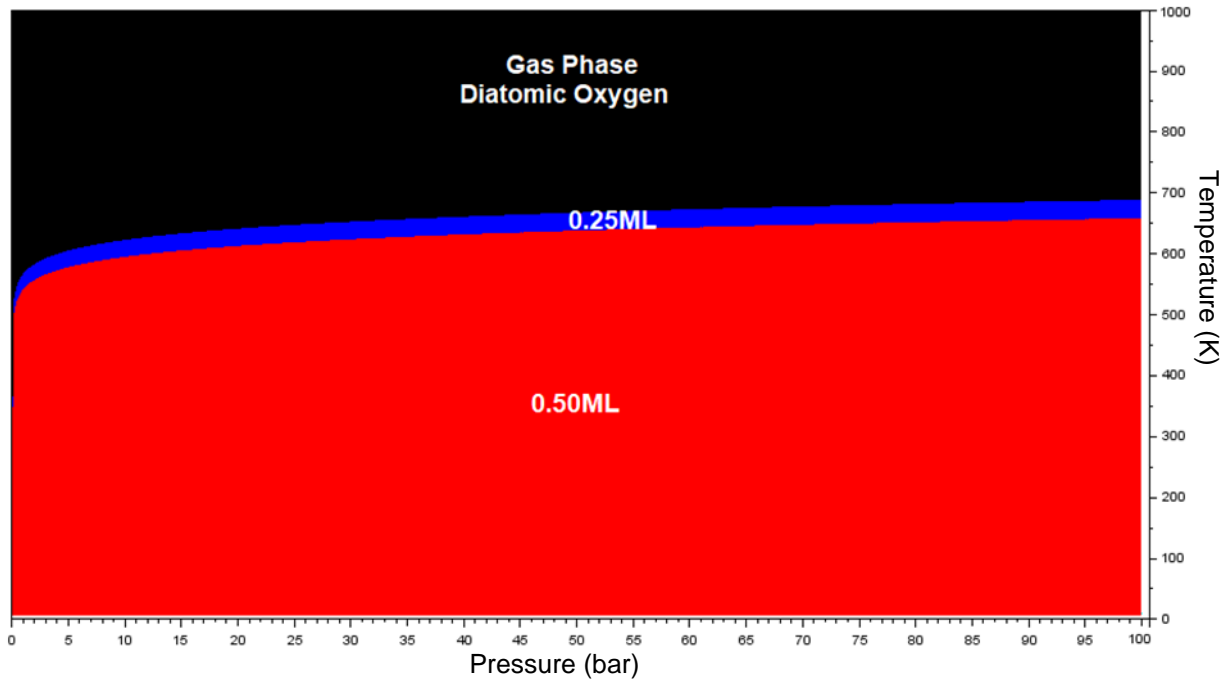


Figure 32: Phase diagram for the adsorption of diatomic oxygen on Pt(100)

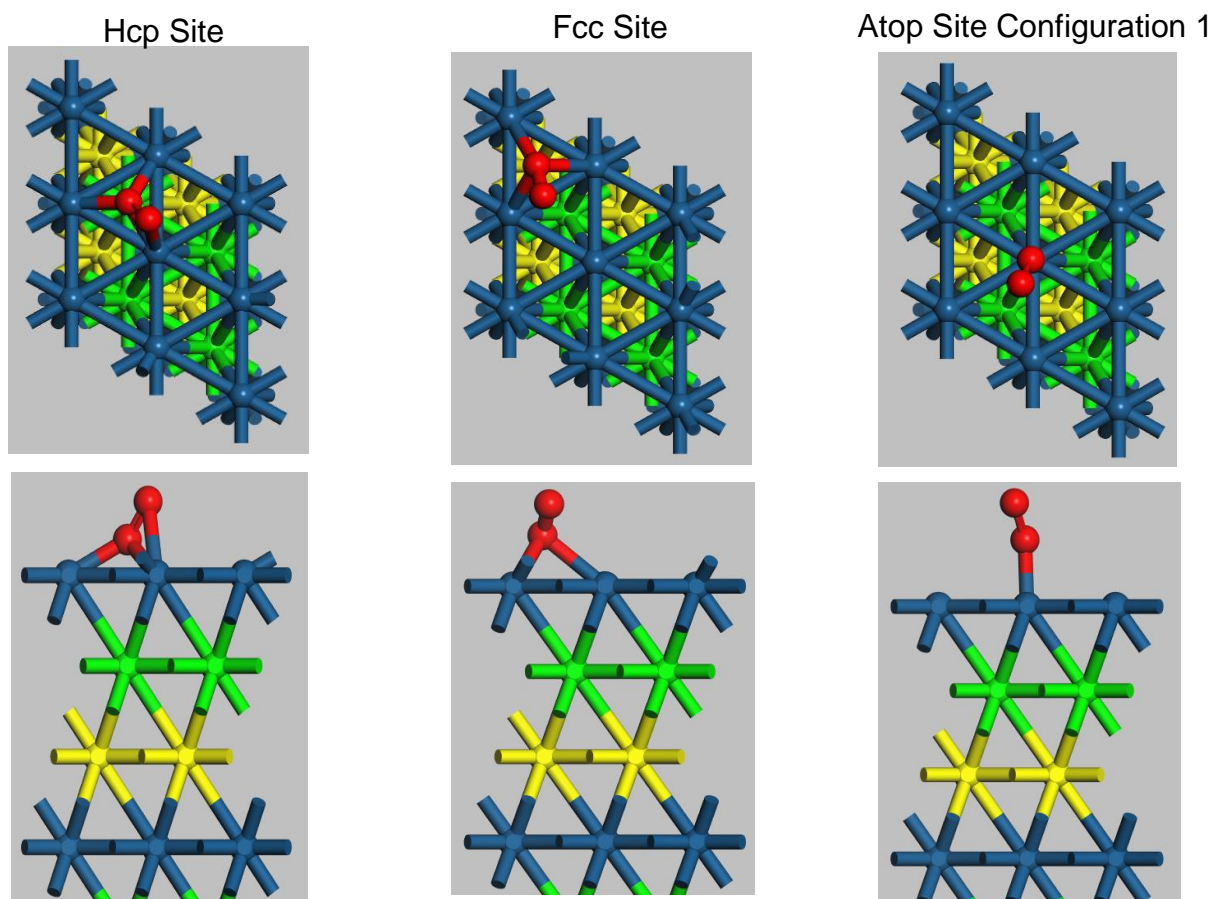
Figure 32 shows the phase diagram for the adsorption of diatomic oxygen on the Pt(100) surface. It can be seen that, at none of the operating conditions under consideration, a coverage of 1.00 ML and 0.75 ML is not obtainable. The highest coverage possible is 0.50 ML and can be obtained at all considered pressures if the temperature is kept below 650 K. There is a small operating range during which a coverage of 0.25 ML is preferred; which is approximately between temperatures of 650 K and 700 K. It must also be noted that the dependence of pressure on the system is very small, and increasing the pressure only allows the system to operate at slightly higher operating temperatures to achieve the same coverage. The main conclusion to be drawn from this phase diagram is that any system involving the adsorption of oxygen on a Pt surface should not operate at temperatures higher than approximately 550 K in order to maximise the adsorption step and not limit the reaction taking place. As any temperature higher than 550 K will result in diatomic oxygen preferring to remain in the gas phase and no adsorption will take place.

## 5. Results and Discussion for Pt(111)

### 5.1 Adsorption Energies and Preferred Adsorption Sites for Pt(111)

#### 5.1.1 Pt(111) at 0.25 ML Coverage

In order to understand the preferred adsorption geometry on the Pt(111) surface, all possible adsorption sites were tested at a coverage of 0.25 ML and their final energies and geometries compared. Due to the three-layer repetition structure of Pt(111), there are four possible sites for adsorption: the bridge site, the atop site, the fcc site and the hcp site; however, each of these adsorption sites have multiple configurations depending on the direction and manner in which the oxygen atoms are adsorbed. Figure 33 below shows the top and side views of the initial geometry of all five systems that were tested at a coverage of 0.25 ML on Pt(111). It must be noted that, in addition to these five configurations, other systems were tested in which the secondary oxygen (that which is not adsorbed on the site of interest) was pointed in other directions; however, these results are not shown as the final geometry of the system was the same regardless of where the second oxygen was pointed. For example: the hcp adsorption site, as seen in Figure 33, has one oxygen atom over the hcp site with the other over an atop site – the same system was tested but with the second oxygen atom facing an fcc site, yielding the exact same final geometry. However, this was only not the case for the atop adsorption site, which is why two configurations for atop adsorption have been reported, as can be seen in Figure 33.



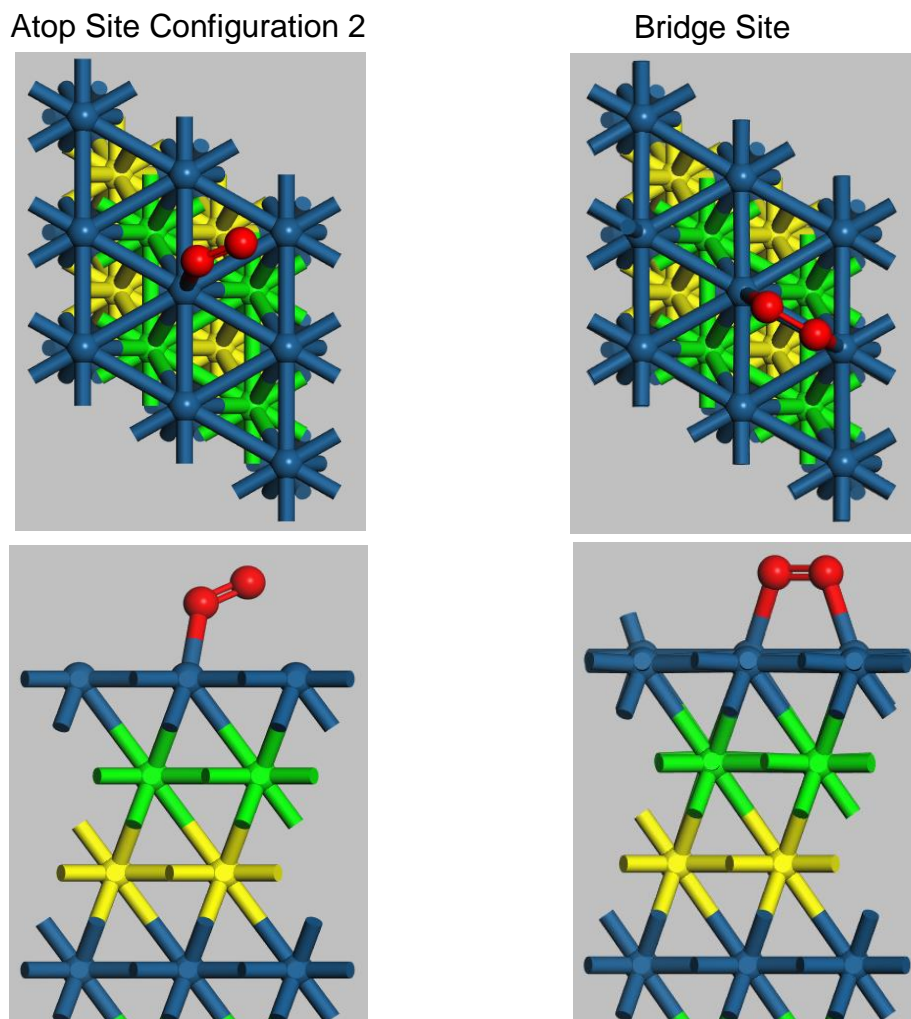
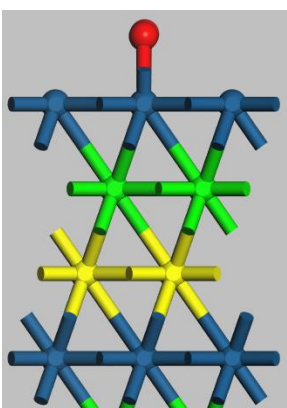
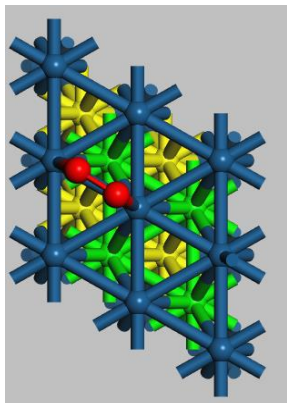


Figure 33: Top (above) and side (below) views of the initial geometries of all five adsorption sites tested at a coverage of 0.25 ML on the Pt(111) surface

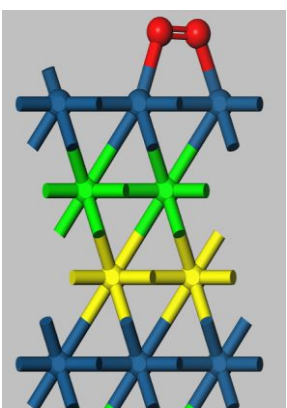
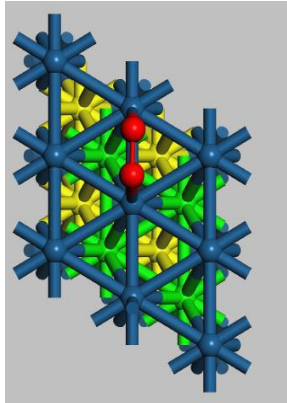
Furthermore, the bridge site is now defined as the same geometry which found to be stable for the Pt(100), which is evident from Figure 33. Additionally, the bond length between the adsorbed oxygen and the Pt surface was kept at a constant 2.00 Å, while the O-O diatomic bond length is kept at a constant 1.35 Å for all initial geometries. Consequently, it can be assumed that comparing the five geometries outlined in Figure 33, while keeping the relevant bond lengths consistent, will lead to the determination of the most preferred adsorption site on Pt(111).

All five configurations, as outlined in Figure 33 above, were run on the *VASP* in order to determine the preferred adsorption site. Figure 34 below gives the top and side views of the final geometries returned by the simulation package for each geometry that was tested. As is clear from Figure 34, all except one of the initial geometries tested ended with bridge site adsorption as its final position, much like for the Pt(100) surface. Only the atop site configuration 2 remained stable over the atop site and did not tend towards the bridge site. Consequently, it can already be confirmed that adsorption of diatomic oxygen over both the fcc and hcp sites on Pt(111) is unstable and will not occur.

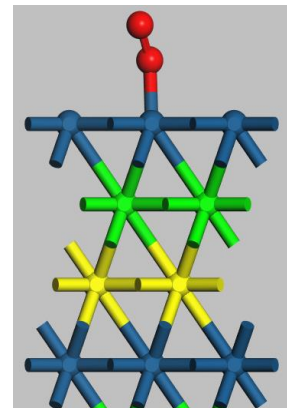
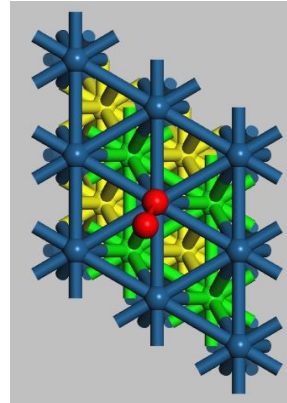
Initial Geometry: Hcp Site  
Final Geometry: Bridge Site



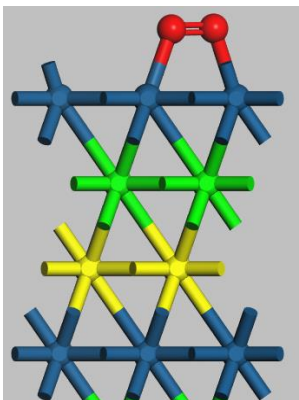
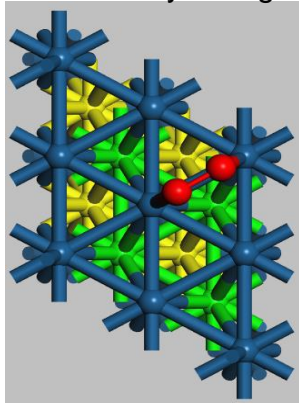
Initial Geometry: Fcc Site  
Final Geometry: Bridge Site



Initial Geometry: Atop Site  
Final Geometry: Atop Site



Initial Geometry: Atop Site  
Final Geometry: Bridge Site



Initial Geometry: Bridge Site  
Final Geometry: Bridge Site

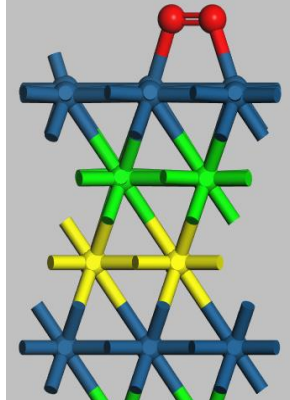
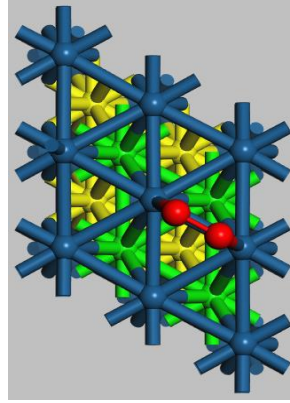


Figure 34: Top (above) and side (below) views of the final geometries of all five adsorption sites tested at a coverage of 0.25 ML on the Pt(111) surface

Table 6: Description of the geometries of all systems tested at a coverage of 0.25ML on the Pt(100) surface and their associated adsorption energies at 0 K

Initial Geometry	Final Geometry	$G_{adsorption}(0K)$
Hcp Site	Bridge Site	-0.60 eV
Fcc Site	Bridge Site	-0.64 eV
Atop Site Configuration 1	Atop Site	-0.30 eV
Atop Site Configuration 2	Bridge Site	-0.64 eV
Bridge Site	Bridge Site	-0.64 eV

The final geometries shown in Figure 34 indicated that both the fcc and hcp adsorption sites were not stable. It can further be deduced from Table 6, which shows the adsorption energies of the systems illustrated in Figure 34, that the atop adsorption site is significantly less stable than the bridge site as it has a much larger adsorption energy. Furthermore, as expected, the adsorption energy for the bridge sites returned identical energies as they all have the same configuration. The initial hcp geometry returned a slightly different adsorption energy; however, this must be due to slight differences in the bond length and configuration in the simulation.

Consequently, it can be concluded that the bridge site, as defined in Figure 34 above, is the most preferred and thermodynamically stable site for the adsorption of diatomic oxygen on Pt(111) at a coverage of 0.25 ML. Considering the highly unstable nature of all other adsorption sites, it can justifiably be assumed that this bridge site will also be preferred at higher coverages and therefore be used as a basis to test the system at higher coverages.

### 5.1.2 Pt(111) at 0.50 ML Coverage

Given that the bridge site was found to be the most stable adsorption geometry at a coverage of 0.25 ML; it is assumed that this site will be preferred at higher coverages. Consequently, all possible configurations of this site were tested at a coverage of 0.50 ML in order to find the most thermodynamically stable system at half coverage. Given that the bridge site was also the most stable for the Pt(100) surface, the same eight configurations of this bridge site at 0.50 ML must be tested, but now on the Pt(111) surface. The initial geometries of all eight configurations that were tested on Pt(111) for 0.50 ML are given in Appendix A1. Table 7 below gives the adsorption energy at 0 K of the final geometry for every stable system of the eight configurations tested. Configuration six evidently has the lowest energy of adsorption and is therefore considered the most stable geometry on Pt(111) at 0.50 ML. The top and side views of the final geometry of configuration six, which represents the preferred adsorption geometry at 0.50 ML, is given in Figure 35.

Table 7: Adsorption energies at 0 K for all eight configurations tested at a coverage of 0.50 ML on the Pt(111) surface

Configuration Number	$G_{adsorption}(0K)$
1	Unstable
2	-0.61 eV
3	-1.07 eV
4	-0.61 eV
5	Unstable
6	-1.13 eV
7	-0.87 eV
8	-0.61 eV

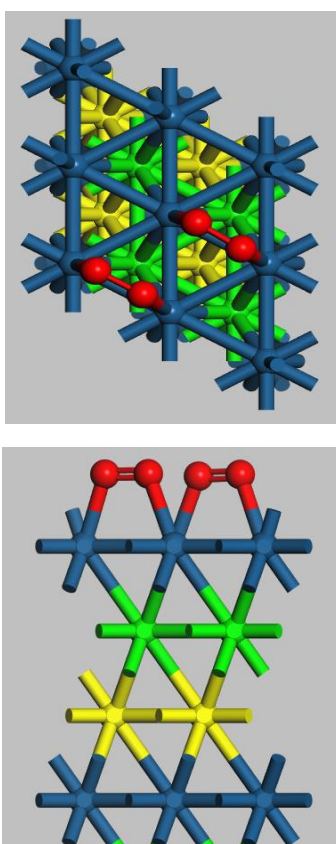


Figure 35: Top (above) and side (below) view of the final geometry of configuration 6 (most stable geometry) at 0.50 ML on the Pt(111) surface

### 5.1.3 Pt(111) at 0.75 ML Coverage

The bridge site is once again assumed to be the preferred adsorption site at 0.75 ML due to the results found at a coverage of 0.25 ML. Consequently, much like for the Pt(100) surface, four configurations of this bridge site at 0.75 ML were tested in order to find the most stable geometry. The top and side views of all four initial geometries tested for Pt(111) at 0.75 ML can be found in Appendix A2.

Table 8: Adsorption energies at 0 K for all four configurations tested at a coverage of 0.75 ML on the Pt(111) surface

Configuration Number	$G_{adsorption}(0K)$
1	Unstable
2	-0.42 eV
3	Unstable
4	-0.50 eV

Table 8 gives the adsorption energies at 0 K for the final geometry of all stable systems of the four configurations that were tested. Both configuration 1 and 3 were unstable, which means that their final geometries did not include three diatomic oxygens adsorbed to the surface, making them inapplicable to understanding the adsorption at a coverage of 0.75 ML. However, both configurations 2 and 4 had final geometries which included all the oxygen molecules initially adsorbed to the surface, and therefore had a coverage of 0.75 ML. Configuration 4 produced the lowest adsorption energy of -0.50 eV, making it the most stable geometry at 0.75 ML coverage. The top and side views of the final geometry of this configuration are shown in Figure 36 below, while the initial geometry can be found in Appendix A2. As can be seen from Figure 36, the oxygen atoms moved away from the bridge site due to strong electronic interactions at this high coverage, which resulted in only one bridge site and two atop adsorption sites.

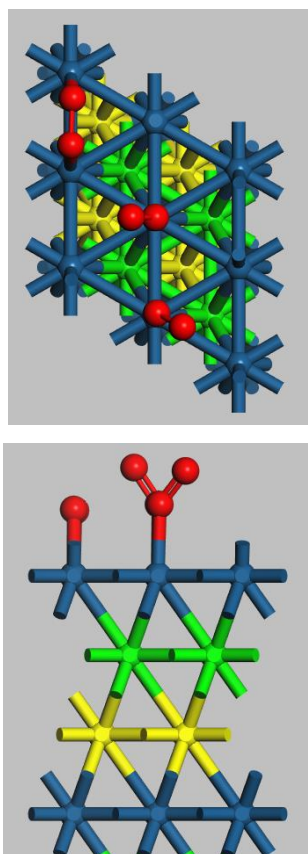


Figure 36: Top (above) and side (below) view of the final geometry of configuration 4 (most stable geometry) at 0.75 ML on the Pt(111)

#### **5.1.4 Pt(111) at 1.00 ML Coverage**

The preferred bridge site used as a basis to test this surface resulted in three possible configurations at a coverage of 1.00 ML, which were all tested in order to understand whether full coverage is stable on Pt(111). The top and side views of the initial geometries of all three configurations that were tested at 1.00ML are shown in Appendix A3. None of the final geometries returned by *VASP* were stable – all three systems tested resulted in desorption of oxygen atoms due to repulsive forces. Consequently, it can be concluded that full coverage of diatomic oxygen on Pt(111) is not possible.

### **5.2 Thermodynamic Analysis of Adsorption of Diatomic Oxygen on Pt(111)**

#### **5.2.1 Overview of Thermodynamics of Adsorption of Diatomic Oxygen on Pt(111)**

It has been found that the bridge site, as defined in Figure 34, is the most stable site for adsorption of diatomic oxygen on Pt(111) at a coverage of 0.25 ML with an associated adsorption energy of -0.64 eV at 0 K. This bridge site was then used as a basis to test for possible stable and preferred geometries at a coverage of 0.50 ML, and it was found that the adsorption of two diatomic oxygen molecules on different bridge sites, as seen in Figure 35, was the most stable at a coverage of 0.50 ML. This adsorption geometry has an associated energy of -1.13 eV at 0 K. The bridge adsorption site was also used to test possible adsorption sites at 0.75 ML; however, the most stable final geometry returned by *VASP* resulted in one diatomic oxygen molecule adsorbed over a bridge site and two diatomic oxygen molecules on separate atop sites, which returned an adsorption energy of -0.50 eV at 0 K. Additionally, it was found that full coverage is not possible on Pt(111).

All of these adsorption energies found using *VASP* are at a temperature of 0 K. It is vital that these energies be calculated over a range of temperatures and pressures in order to gauge what geometry will be present on the Pt(111) surface at a specific set of operating conditions. This was done by conducting a vibrational analysis on the final geometry of the most stable system at each coverage in conjunction with the thermodynamic correlations described in Section 3.10 to reevaluate the energies at varying operating conditions.

#### **5.2.2 Dependence of the Adsorption Geometry on Temperature on Pt(111)**

The Gibbs energy of adsorption for each coverage was calculated at 1 atm at temperatures ranging from 0 K to 1000 K. This was done in an effort to illustrate the preferred adsorption geometry on Pt(111) over a range of temperatures by comparing the Gibbs energy of adsorption for each coverage; the lowest of which represents the

most stable system. From Figure 37 below, it is clear that there is no temperature at 1 atm at which a coverage of 0.75 ML is stable on Pt(111). The most stable system at each temperature is represented by the system with the lowest Gibbs energy of adsorption, as long as this energy is negative. If all the adsorption energies are positive, it means that adsorption onto the surface is non-spontaneous and oxygen will prefer to remain in the gas phase. As is evident from Figure 37, at low temperatures and 1 atm, a coverage of 0.50 ML is preferred on the surface.

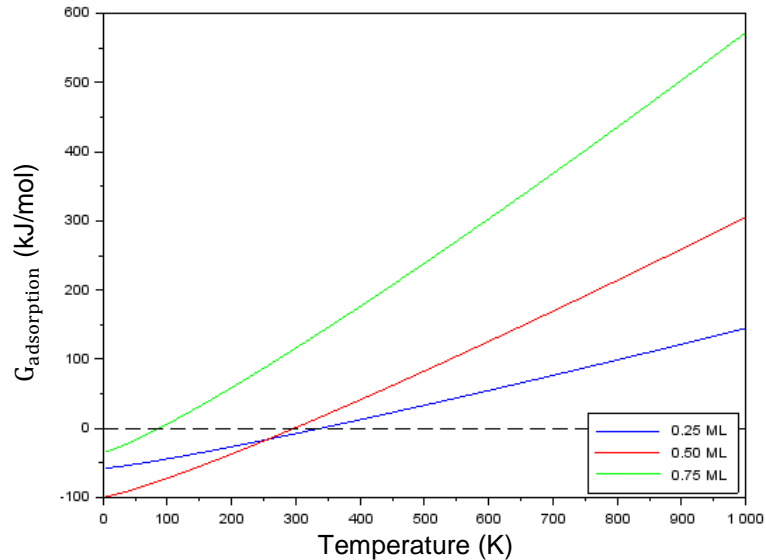


Figure 37: Gibbs energy of adsorption at 1 atm for all three possible coverages on Pt(111) over a range of temperatures

A coverage of 0.50 ML is thermodynamically preferred on the surface at 1 atm from 0 K until 255 K, as is clear from Figure 38, which represents a zoomed in view of Figure 37. Between 255 K and 337 K, a coverage of 0.25 ML is preferred; therefore, if two diatomic oxygen molecules were available above the surface, at 1 atm and within this temperature range, only one would adsorb. At any temperature higher than 337 K, the Gibbs energy of adsorption of all three possible coverages is positive; hence, diatomic oxygen would not adsorb on Pt(111).

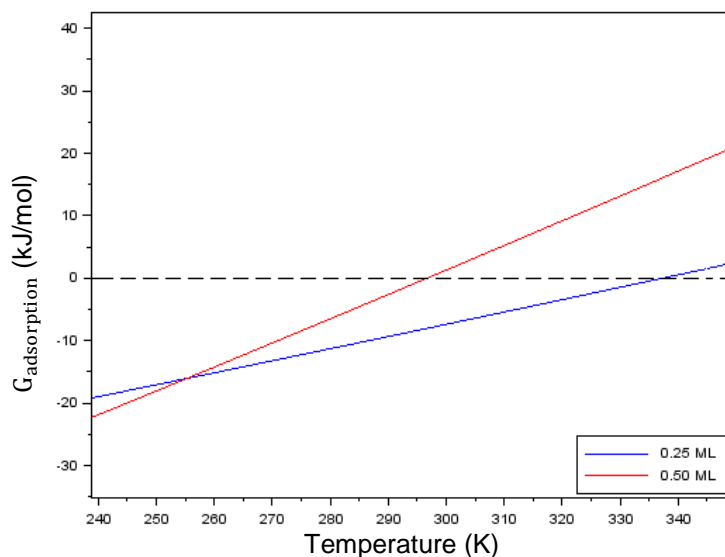


Figure 38: Zoomed in view of the Gibbs energy of adsorption at 1 atm for all three possible coverages on Pt(111) over a range of temperatures

### 5.2.3 Dependence of the Adsorption Geometry on Pressure on Pt(111)

The dependence of pressure on the Gibbs energy of adsorption for each coverage was tested at a constant temperature of 25 °C. The Gibbs energy of adsorption was calculated, at this constant temperature, between 0 bar and 100 bar in order to illustrate the preferred adsorption system at various pressures, as is shown in Figure 39. As is clear from Figure 39, the Gibbs energy of adsorption for a coverage of 0.75 ML is always positive at 25 °C, regardless of the pressure. Consequently, this coverage will never be thermodynamically stable at these conditions and 0.75 ML will not be possible on Pt(111). Between 0 bar and 27 bar, a coverage of 0.25 ML is the most stable on Pt(111) at 25 °C, as shown in Figure 39. At any pressure higher than 27 bar, a coverage of 0.50 ML is favoured and the Gibbs energy of adsorption remains negative. Therefore, at 25°C, adsorption of diatomic oxygen onto Pt(111) will take place at all reasonable pressures, as the adsorption energy of any of the coverages is always negative, with adsorption at 0.50 ML favoured at pressures higher than 27 bar.

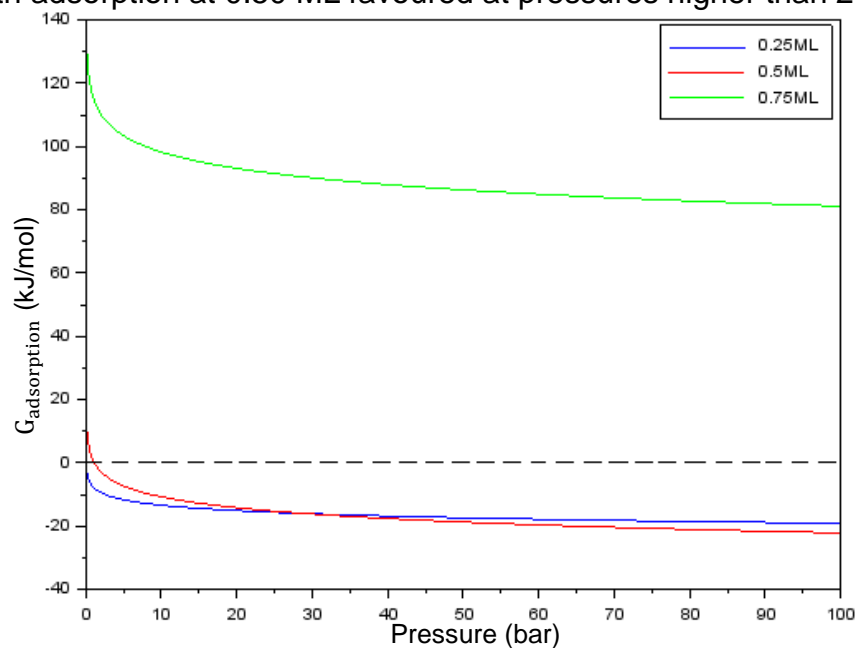


Figure 39: Gibbs energy of adsorption at 25 °C for all three possible coverages on Pt(111) over a range of pressures

### 5.3 Phase Diagram for the Adsorption of Diatomic Oxygen on Pt(111)

In order to evaluate the operating conditions at which particular coverages are possible, the temperature and pressure dependence of the Gibbs energy of adsorption was incorporated into a three-dimensional plot to simultaneously track their influence on the system. A side view of this three-dimensional plot is given in Figure 40 below, in order to illustrate how the Gibbs energy of adsorption for each coverage changes by simultaneously varying the system's temperature and pressure.

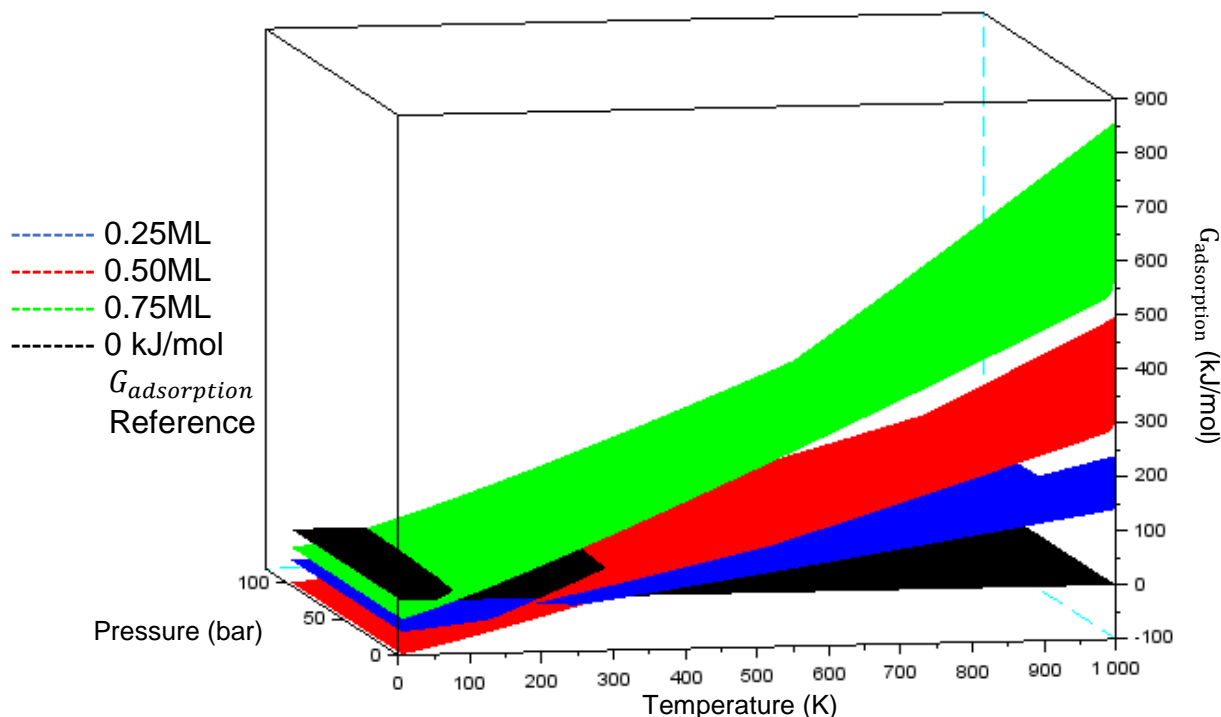


Figure 40: Side view of the three-dimensional plot of all interacting surfaces used to develop the phase diagram for Pt(111)

The most preferred geometry at a certain set of conditions is represented by the system with the lowest Gibbs energy of adsorption. Consequently, the part of this three-dimensional plot of interest will always be the lowest surface at specific conditions. Therefore, a phase diagram was developed by viewing this three-dimensional plot from the bottom in order to illustrate the system with the lowest Gibbs energy of adsorption at any conditions. This phase diagram for Pt(111) is given in Figure 41 below.

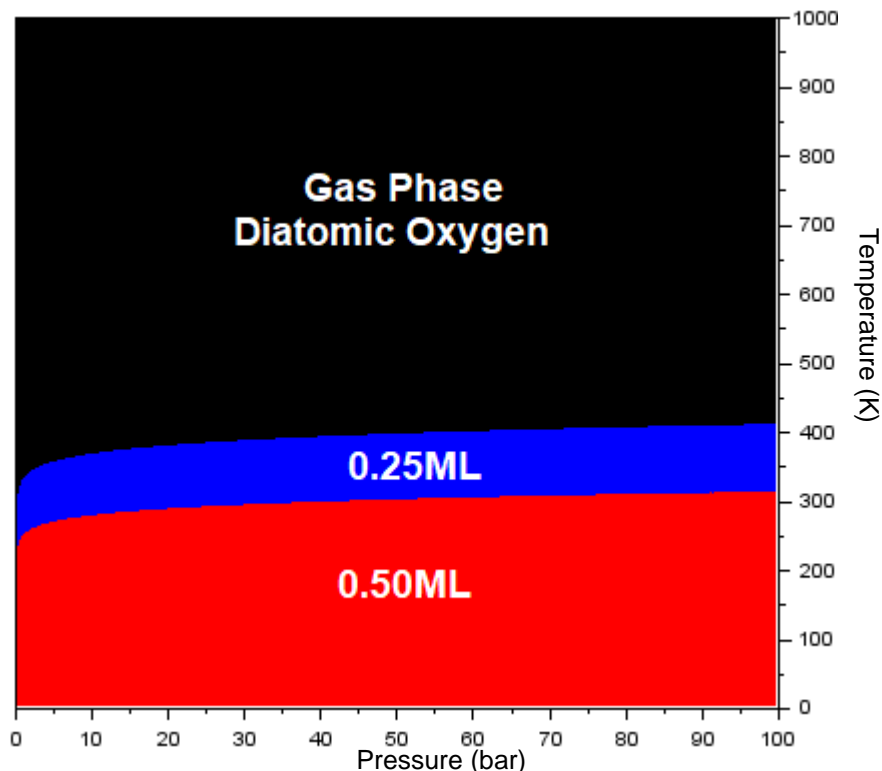


Figure 41: Phase diagram for the adsorption of diatomic oxygen on Pt(111)

As is evident from the phase diagram in Figure 41, there is no set of operating conditions within the tested range of 0-100 bar and 0-1000 K at which a coverage higher than 0.50 ML is obtainable on Pt(111). It was found that increasing the system's pressure always allows the same coverage to be obtained at a slightly higher temperature. Furthermore, for all given pressures, a coverage of 0.50 ML can be obtained at temperatures lower than approximately 300 K. Additionally, there is an operating range between approximately 300-400 K in which a coverage of 0.25ML is favoured; while at temperatures higher than 400 K diatomic oxygen prefers to remain in the gas phase rather than adsorbing on the surface, at all pressures. This phase diagram represents the preferred adsorption configuration on Pt(111) over any reasonable operating pressures and temperatures; and can therefore be used to optimise operating conditions in a Pt catalysed reaction system.

## Conclusion

In order to determine the most stable adsorption geometries of diatomic oxygen and their associated energies on the Pt(100) and Pt(111) surfaces, the system was modelled using *VASP*. This simulation iterated the total energy of the system, from a specified initial geometry, until an energy minimum is achieved. Consequently, the stability and energy of all possible adsorption sites was tested at varying coverages and their energies compared in order to understand which adsorption geometry is the most stable.

Initial geometries of a diatomic oxygen adsorbed over an hcp, atop and bridge site were all tested for Pt(100) at 0.25 ML. It was found that all three systems tended towards bridge site adsorption; consequently, only the bridge site was found to be stable on this surface. This particular configuration of bridge site adsorption involved both oxygen atoms adsorbed over the same bridge site while still diatomically bonded, and had an adsorption energy on Pt(100) of -1.14 eV at 0 K. It was then assumed that this bridge site was the most stable at higher coverages and possible configurations of this bridge site adsorption were used as initial geometries to test the system at coverages of 0.50 ML, 0.75 ML and 1.00 ML. At a coverage of 0.50 ML, the adsorption remained most stable on this bridge site with an adsorption energy of -2.24 eV. At a coverage of 0.75 ML, the most stable adsorption geometry involved two oxygen atoms dissociating and adsorbing on two separate bridge sites, with the other two diatomic oxygens adsorbed to two separate atop sites. This represented the most stable adsorption geometry at 0.75 ML and had an adsorption energy of -2.13 eV. It was found that the adsorption of diatomic oxygen on Pt(100) at full coverage was never stable, despite testing multiple configurations of bridge site adsorption. Consequently, there are no conditions at which full coverage can be obtained on this surface.

A phase diagram was created for the adsorption of diatomic oxygen on Pt(100) in order to understand how the most stable system geometry changes over a range of operating temperatures and pressures. This was done by conducting a vibrational analysis on the most stable system for each coverages and then using thermodynamic correlations to calculate the Gibbs energy of adsorption at various operating conditions. It was found that there are no operating conditions between 0-1000 K and 0-100 bar at which a coverage higher than 0.50 ML is favoured. Over all the tested pressures, a coverage of 0.50 ML can be achieved if the temperature is kept below 500 K. If the temperature is increased, there is a small operating region in which a coverage of 0.25 ML is the most favoured geometry. However, for the entire pressure range tested, if the temperature of the system is higher than 700 K then no oxygen will adsorb on the surface, as it will rather prefer to remain in the gas phase.

A similar procedure was carried out to investigate the adsorption of diatomic oxygen on Pt(111). Firstly, initial geometries on the fcc, hcp, atop and bridge sites were tested at a coverage of 0.25 ML in order to determine the most stable adsorption site. The fcc and hcp sites were found to be unstable, and they both produced final geometries that

were the same as the bridge adsorption geometry for the Pt(100) surface. The atop site remained stable, but returned a larger adsorption energy than the bridge site adsorption, making it less thermodynamically stable. Consequently, the bridge site adsorption was also found to be preferred on Pt(111) at 0.25 ML, and has an associated adsorption energy of -0.64 eV at 0 K. This bridge adsorption site remained stable at a coverage of 0.50 ML and returned an adsorption energy of -1.13 eV at 0 K. At a coverage of 0.75 ML, it was found that the most stable geometry involved the bridge site adsorption of one of the diatomic oxygen with the other two adsorbed on atop sites. This adsorption geometry reported an adsorption energy of -0.50 eV at 0 K. It was found that full coverage is also not possible on the Pt(111) surface as no stable geometries were determined.

A phase diagram was also developed for the Pt(111) surface in order to illustrate the operating conditions at which certain geometries are preferred. The operating range of this diagram is the same as that for the Pt(100) phase diagram: 0-1000 K and 0-100 bar. It was once again found that no coverage higher than 0.50 ML can be obtained given these operating ranges. Furthermore, this coverage is only achievable at temperatures lower than 300 K. In general, slightly higher temperatures can achieve the same coverage if the pressure is increased, but pressure has a significantly smaller influence on the Gibbs energy of adsorption than temperature. The operating range of 0.25 ML is much larger for Pt(111) compared to the Pt(100) surface, with this coverage being the most stable approximately between 300 K and 400 K. At any temperature higher than 420 K, at all pressures under consideration, diatomic oxygen will not adsorb on the Pt(111) surface.

In conclusion, the most stable adsorption configurations and their associated energies at coverages of 0.25 ML, 0.50 ML and 0.75 ML were found for both the Pt(100) and Pt(111) surfaces. It was also determined that neither surface is stable at full coverage of diatomic oxygen and therefore a coverage of 1.00 ML cannot be obtained. The highest obtainable coverage, within a range of reasonable operating conditions, is 0.50 ML for both surfaces. The phase diagrams for both surfaces were developed in order to simultaneously track the effect of temperature and pressure on the Gibbs energy of adsorption of each coverage in order to determine the most preferred surface configuration given a set of operating conditions.

## References

- Arblaster, B. 1997. Crystallographic Properties of Platinum. *Platinum Metals Rev.* 41(1): 12–21.
- Barbir, F. 2005. PEM Electrolysis for Production of Hydrogen from Renewable Energy Sources. *Solar Energy.* 78(2005): 661-669.
- British Petroleum. 2013. BP Energy Outlook 2030. London.
- British Petroleum. 2016. BP Statistical Review of World Energy. London.
- Car, R. & Parrinello, M. 1985. Unified Approach for Molecular Dynamics and Density-Functional Theory. *Physical Review Letters.* 55(22): 2471-2474.
- Fiorin, V., Borthwick, D. & King, D. A. 2009. Microcalorimetry of O<sub>2</sub> and NO on Flat and Stepped Platinum Surfaces. *Surface Science.* 603 (2009): 1360-1364.
- Ford, D.C. Xu, Y. & Mavrikakis, M. 2005. Atomic and Molecular Adsorption on Pt(111). *Surface Science.* 587(2005): 159-174.
- Foster, N. 1985. Direct Catalytic Oxidation of Methane to Methanol – A Review. *Applied Catalysis.* 19(1985): 1-11.
- Fratesi, G., Gava, P. & Gironcoli, S. 2007. Direct Methane-to-Methanol Conversion: Insight from First-Principles Calculations. *Journal of Physical Chemistry.* 111(2007): 17015-17019.
- Gesser, H., Hunter, N. & Prakash, C. 1985. The Direct Conversion of Methane to Methanol by Controlled Oxidation. *Chemical Reviews.* 85(4): 235-244.
- Gland, J. L. Sexton, B. A. & Fisher, G. B. 1980. Oxygen Interactions with the Pt(111) Surface. *Surface Science.* 95(1980): 587-602.
- Gray, H.B. 1994. *Chemical Bonds: An Introduction to Atomic and Molecular Structure.* Mill Valley, California: University Science Books.
- Green, D. & Perry, R. *Perry's Chemical Engineers' Handbook.* 8th ed. University of Kansas: McGraw-Hill, 2008.
- Gu, Z. & Balbuena, P. 2007. Absorption of Atomic Oxygen into Subsurfaces of Pt(100) and Pt(111): Density Functional Theory Study. *Journal of Physical Chemistry.* 111(2007): 9877-9883.
- Hermann, K. 2011. *Crystallography and Surface Structure: An Introduction for Surface Scientists and Nanoscientists.* Wiley.
- Hirano, T. 1993. *MOPAC Manual.* 7<sup>th</sup> ed. Stewart, J. J. P.

Karp, E. M., Campbell, C. T., Studt, F., Abild-Pedersen, F. & Norskov, J. K. 2012. Energetics of Oxygen Adatoms, Hydroxyl Species and Water Dissociation on Pt(111). *The Journal of Physical Chemistry*. 116: 25772–25776.

Liu, H., Song, C., Zhang, L., Zhang, J., Wang, H. & Wilkinson, D. 2006. A Review of Anode Catalysis in the Direct Methanol Fuel Cell. *Journal of Power Sources*. 155(2006): 95-110.

Lynch, M. & Hu, P. 2000. A Density Functional Theory Study of CO and Atomic Oxygen Chemisorption on Pt(111). *Surface Science*. 458(2000): 1-14.

Memorial University Department of Chemistry. 2017. Vibrational Frequencies of Atmospheric Gases.

Available: <http://www.chem.mun.ca/homes/cnrhome/vibration/o2-vib.html> [2017, November 21]

Norskov, J., Rossmeisl, J., Logadottir, A., Lindqvist, L., Kitchin, J., Bligaard, T. & Jonsson, H. 2004. Origin of the Overpotential for Oxygen Reduction at a Fuel-Cell Cathode. *Journal of Physical Chemistry*. 108(2004): 17886-17892.

Puglia, C., Nilsson, A., Hernnas, B., Karis, O., Bennich, P. & Martensson, N. 1995. Physisorbed, Chemisorbed and Dissociated O<sub>2</sub> on Pt(111) Studied by Different Core Level Spectroscopy Methods. *Surface Science*. 342(1995): 119-133.

Reed, T. & Lerner, R. 1973. Methanol: A Versatile Fuel for Immediate Use. *Science*. 182(4119): 1299-1304.

Sandler, S. I. 2006. *Chemical, Biochemical, and Engineering Thermodynamics*. 4th ed. Delaware: John Wiley & Sons.

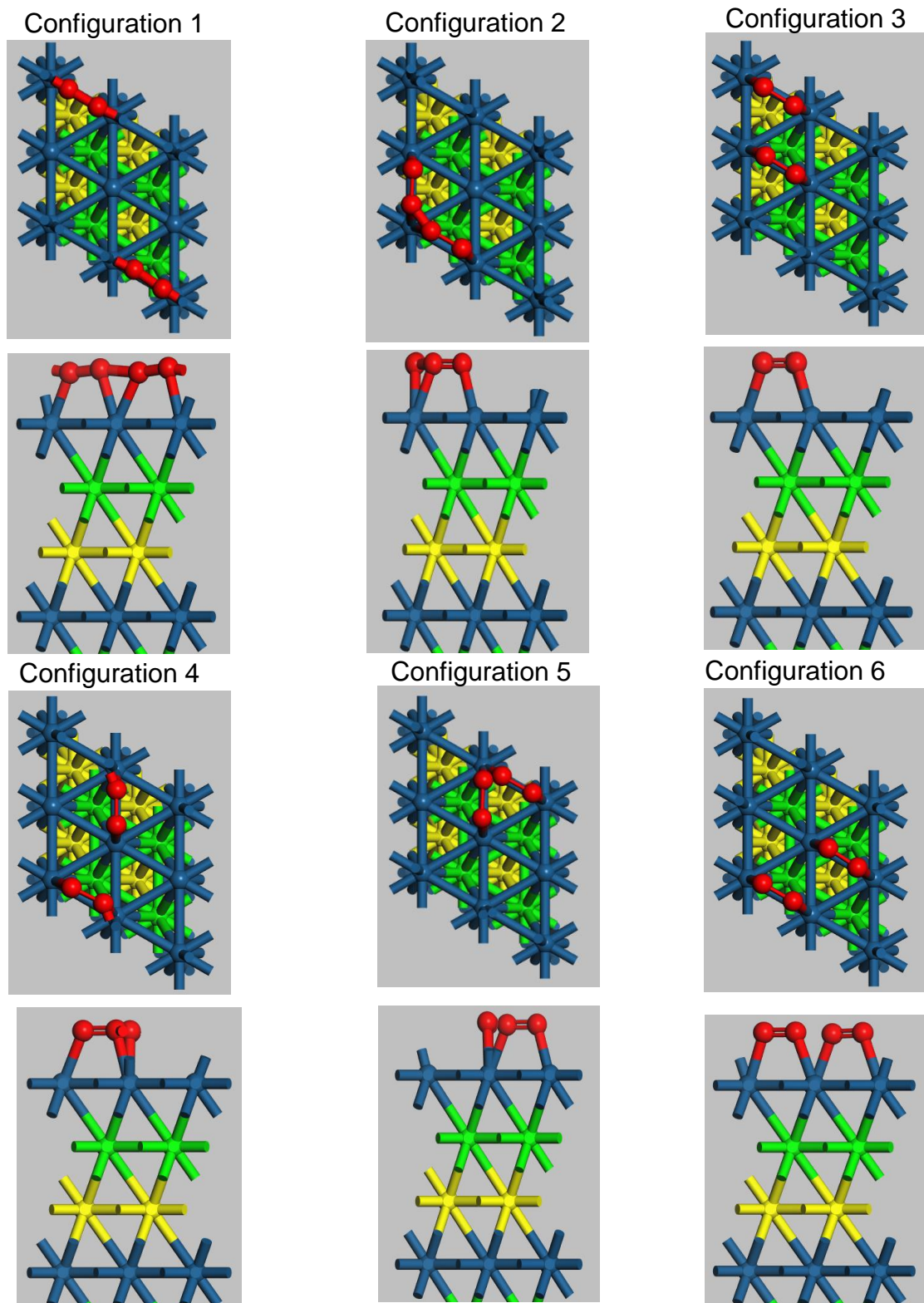
Tripkovic, V., Cerri, I., Bligaard, T. & Rossmeisl, J. 2014. The Influence of Particle Shape and Size on the Activity of Platinum Nanoparticles for Oxygen Reduction Reaction: A Density Functional Theory Study. *Catalysis Letters*. 144(2014): 380-388.

Xu, X. & Goddard, W.A. 2004. The Extended Perdew-Burke-Ernzerhof Functional with Improved Accuracy for Thermodynamic and Electronic Properties of Molecular Systems. *Journal of Chemical Physics*. 121(9): 4068-4082.

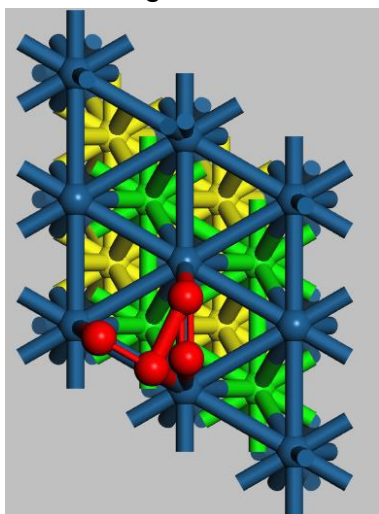
## Appendices

### Appendix A: Top and Side Views of the Initial Geometries for All Systems Tested for Pt(111)

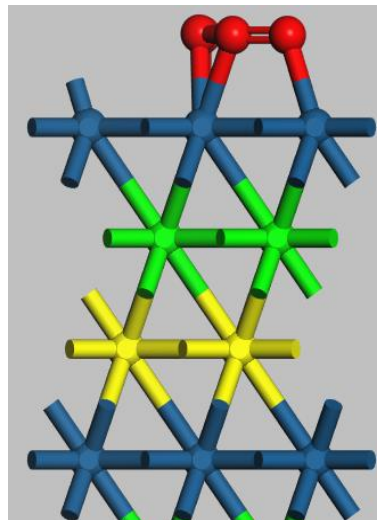
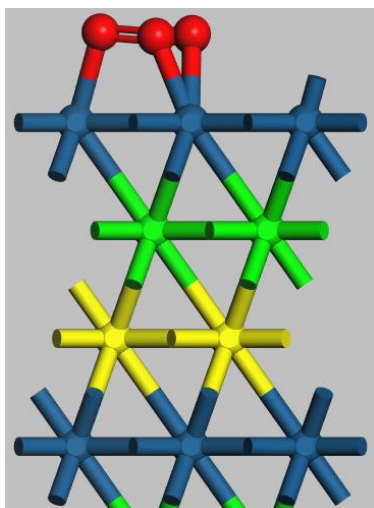
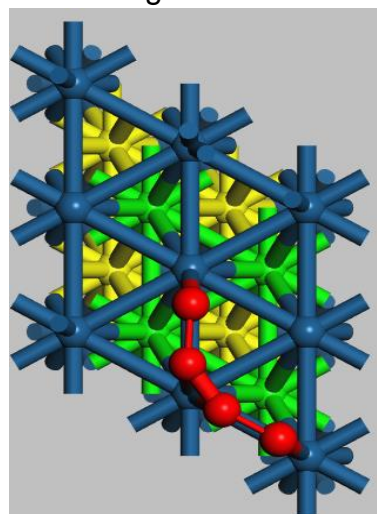
#### Appendix A1: Top and Side Views of the Initial Geometries for All Systems Tested for Pt(111) at 0.50 ML Coverage



Configuration 7

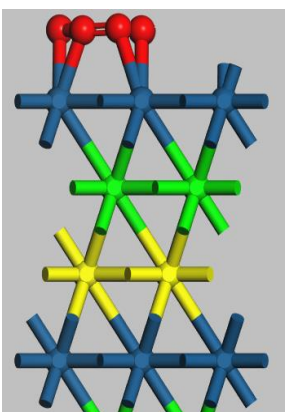
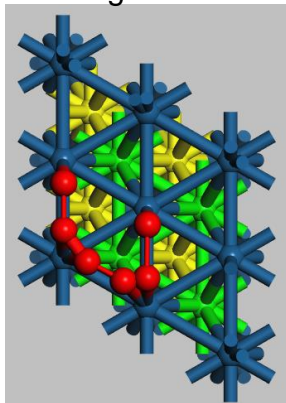


Configuration 8

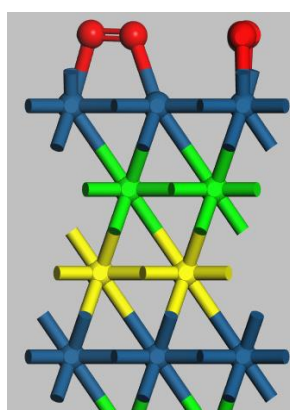
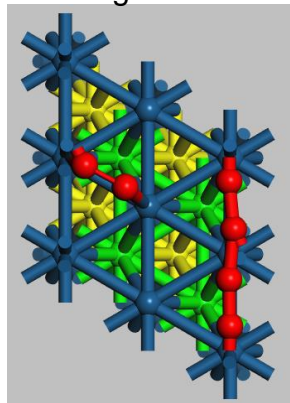


## Appendix A2: Top and Side Views of the Initial Geometries for All Systems Tested for Pt(111) at 0.75 ML Coverage

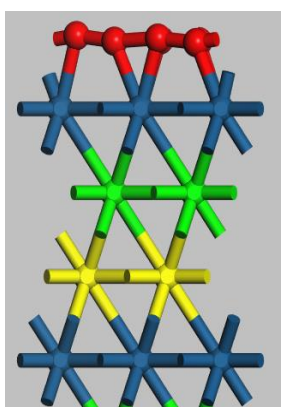
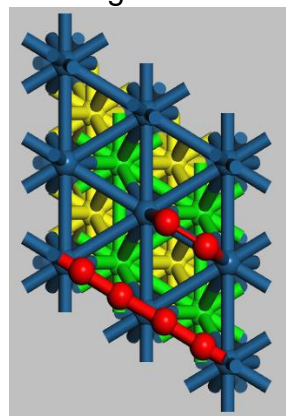
Configuration 1



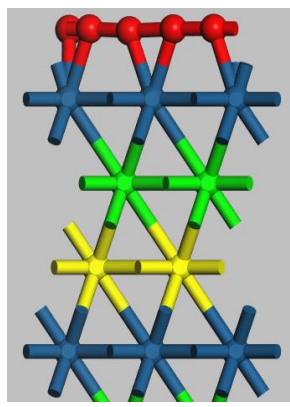
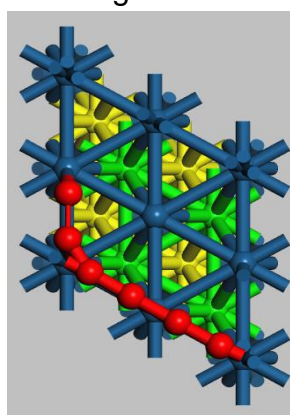
Configuration 2



Configuration 3

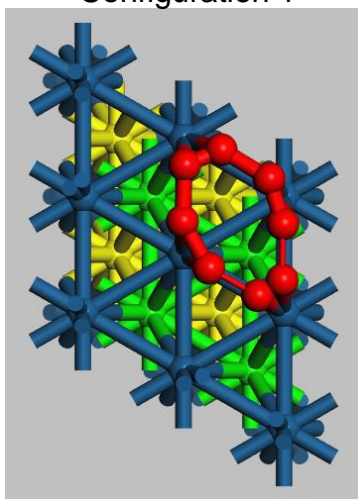


Configuration 4

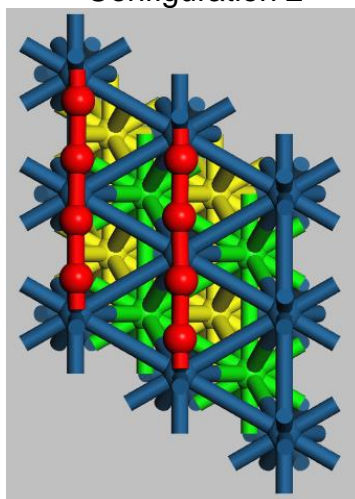


### Appendix A3: Top and Side Views of the Initial Geometries for All Systems Tested for Pt(111) at 1.00 ML Coverage

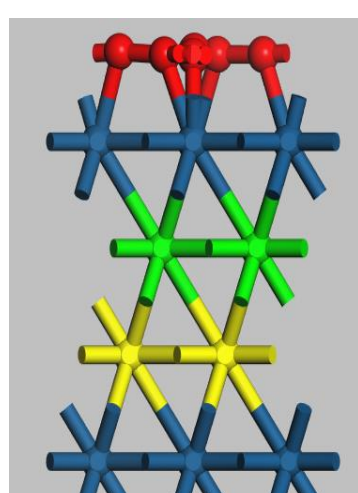
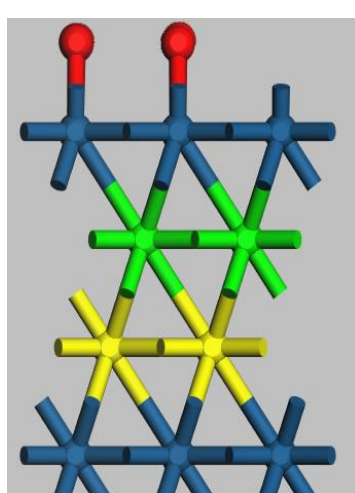
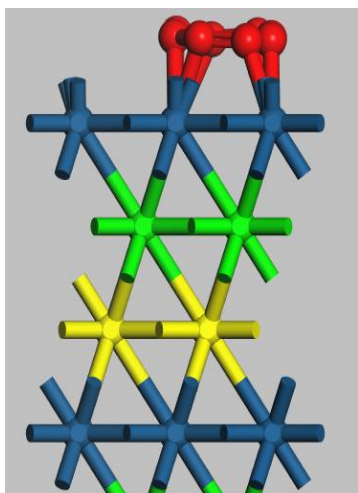
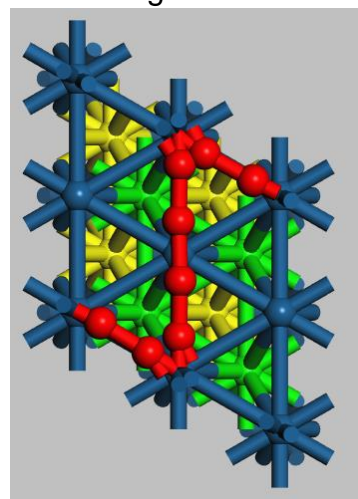
Configuration 1



Configuration 2



Configuration 3



## **Appendix C: Ethical Considerations**

### **Appendix C1: Cover Letter for EBE Ethical Research Application**

Dear Sir/Madame,

Our names are Jean-Claude Carreno and Michel Amato and we are two 4<sup>th</sup> year chemical engineering students currently enrolled for our 4<sup>th</sup> year final projects as part of the CHE4045Z course at the University of Cape Town. This letter is to serve as an official cover letter to accompany our EBE Ethics Application for our research project. Our research project is titled 'A DFT Study of Diatomic Oxygen Adsorption on Pt(100) and Pt(111)'. This project is to be supervised by the chemical engineering head of department Eric Van Steen, as well as lecturer Tracey Van Heerden and masters student Pierre Cilliers. The study will use computational simulation to investigate the adsorption of oxygen on a platinum surface. The study is entirely computer based and makes use of a number of software resources provided by the department of chemical engineering, as well as the computing power of the UCT ICTS HPC supercomputer and the UCT chemical engineering department Chimera supercomputer. The study serves to expand upon the existing masters work of Pierre Cilliers. The project proposal with an in depth explanation on the proposed work surrounding this project has been attached with this letter.

Ethical considerations surrounding the nature of the work conducted within the project have been considered. Research to be conducted within the proposed dissertation is to be done in a manner which adheres to the rules and regulations of the University of Cape Town as outlined in the General Rules and Policies handbook, as well as to the integrity and respect for others expected within the Republic of South Africa as outline in the Constitution.

#### **The following ethical issues have been identified within the proposed project:**

Work conducted within the proposed thesis requires extensive resources including access to the Chimera supercomputer server belonging to the Chemical Engineering Department in the University of Cape Town as well as the HPC supercomputer belonging to ICTS. Further resources include various papers and past works which are accessible through the libraries of the university and various software resources licensed through the university. Furthermore, the proposed dissertation serves to continue the existing work of the university, lead by Pierre Cilliers (Bsc.Eng Chemical) and Professor Eric Van Steen (PhD.Eng Chemical), whereby extensive access to the existing information from this work will be required.

**In order to ensure ethical conduction of the proposed dissertation, the following principles will be upheld:**

- Proper acknowledgment of previous work conducted by various other authors where appropriate
- Appropriate conduction of Chimera and HCP supercomputer usage whereby these valuable resources are used exclusively to further the work of the proposed dissertation with no personal use
- Consideration of other researchers when accessing Chimera server with no abuse of access
- Professional and appropriate conduct around all involved in the creation of the propose dissertation
- Honest and accurate reporting of results with no conflict of interest or personal agenda in reporting
- Safe conduct when moving around the Chemical Engineering building at the University of Cape Town with awareness of other researchers and respect for the space, as well as awareness of the safety procedures to be followed within the building

**The following have been considered within the proposed research project:**

- No testing on humans or animals
- No health or safety impacts on society
- No use of minors within the study
- No use of private or sensitive information
- No conflicts of interest in the research which may compromise results
- No placement of researchers at risk

**Safety, Health and Environmental Considerations**

Consideration on the health and safety of all involved in the creation of the proposed dissertation, as well as the environmental impact of the proposed work is central to all research and to the code of morals upheld by all South African engineers as reinforced in the Engineering Council of South Africa (ECSA) Code of Conduct. Conduction of work in a manner which ensures the inherent health and safety of all directly and indirectly involved as outlined in Section 3.3 of the ECSA Code of Conduct, as well as ensuring minimal environmental impact as outlined in Section 3.4, is central to the operation of all engineering based research. The proposed dissertation is limited to the usage of software where experimental results are obtained through simulation, thus limiting the risk of health and safety to society, as well as limiting environmental impact through no need to use physical materials other than electrical requirements to run the software.

We hope that the information within this letter and the accompanying project proposal are sufficient for the granting of the EBE Ethical Application for our project. Please feel free to contact us if there are any more information regarding ethical considerations we may provide.

Regards,

Jean-Claude Carreno

[CRRJEA003@myuct.ac.za](mailto:CRRJEA003@myuct.ac.za)

Michel Amato

[AMTMIC001@myuct.ac.za](mailto:AMTMIC001@myuct.ac.za)

## Appendix C2: EBE Ethical Research Application Form

Application for Approval of Ethics in Research (EIR) Projects  
Faculty of Engineering and the Built Environment, University of Cape Town

### APPLICATION FORM

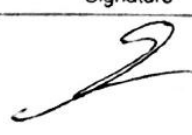
**Please Note:**

Any person planning to undertake research in the Faculty of Engineering and the Built Environment (EBE) at the University of Cape Town is required to complete this form **before** collecting or analysing data. The objective of submitting this application *prior* to embarking on research is to ensure that the highest ethical standards in research, conducted under the auspices of the EBE Faculty, are met. Please ensure that you have read, and understood the EBE Ethics in Research Handbook (available from the UCT EBE, Research Ethics website) prior to completing this application form: <http://www.ebe.uct.ac.za/ebe/research/ethics1>

APPLICANT'S DETAILS		
Name of principal researcher, student or external applicant		Jean-Claude Carreno and Michel Amato
Department		UCT Chemical Engineering
Preferred email address of applicant:		CRRJEA003@myuct.ac.za
If Student	Your Degree: e.g., MSc, PhD, etc.	Bsc Eng Chemical
	Credit Value of Research e.g., 60/120/180/360 etc.	36
	Name of Supervisor (if supervised):	Professor Eric Van Steen
If this is a research contract, indicate the source of funding/sponsorship		Click here to enter text.
Project Title		A DFT Study of Diatomic Oxygen Adsorption on Pt(100) and Pt(111)

**I hereby undertake to carry out my research in such a way that:**

- there is no apparent legal objection to the nature or the method of research; and
- the research will not compromise staff or students or the other responsibilities of the University;
- the stated objective will be achieved, and the findings will have a high degree of validity;
- limitations and alternative interpretations will be considered;
- the findings could be subject to peer review and publicly available; and
- I will comply with the conventions of copyright and avoid any practice that would constitute plagiarism.

SIGNED BY	Full name	Signature	Date
Principal Researcher/ Student/External applicant	Jean-Claude Carreno		09 Nov 2017
	Michel Amato		09 Nov 2017
APPLICATION APPROVED BY	Full name	Signature	Date
Supervisor (where applicable)	Professor Eric Van Steen		09 Nov 2017
HOD (or delegated nominee) Final authority for all applicants who have answered NO to all questions in Section 1; and for all Undergraduate research (Including Honours).	Professor Eric Van Steen		09 Nov 2017
Chair : Faculty EIR Committee For applicants other than undergraduate students who have answered YES to any of the above questions.			

## Appendix D: Plagiarism Declaration Form



### DEPARTMENT OF CHEMICAL ENGINEERING

UNIVERSITY OF CAPE TOWN

CHE4045Z

Chemical Engineering Project

<b>2017</b>			
<b>Student Numbers</b>	CRRJEA003    AMTMIC001		
<b>Date Completed</b>	23/11/2017	<b>Date Handed-In</b>	23/11/2017
<b>DECLARATION</b>			
1. I know that plagiarism is wrong. Plagiarism is to use another's work and to pretend that it is one's own. 2. This report is my own work. 3. I have not allowed, and will not allow, anyone to copy this work with the intention of passing it off as his or her own work.			
<b>Signatures</b>	<b>Jean-Claude Carreno</b>		
	<b>Michel Amato</b>		